ANKARA YILDIRIM BEYAZIT UNIVERSITY

GRADUATE SCHOOL OF NATURAL AND APPLIED SCIENCES

NUMERICAL INVESTIGATION OF A SLIDER CANOPY LOCKING MECHANISM

M.Sc. Thesis by

Furkan İPEKOĞLU

Department of Mechanical Engineering

November 2024

ANKARA

NUMERICAL INVESTIGATION OF A SLIDER CANOPY LOCKING MECHANISM

A Thesis Submitted to

The Graduate School of Natural and Applied Sciences of

Ankara Yıldırım Beyazıt University

In Partial Fulfillment of the Requirements for the Degree of Master of Science in Mechanical Engineering, Department of Mechanical Engineering

by

Furkan İPEKOĞLU

November 2024

ANKARA

M.Sc. THESIS EXAMINATION RESULT FORM

We have read the thesis entitled **"NUMERICAL INVESTIGATION OF A SLIDER CANOPY LOCKING MECHANISM"** completed by **FURKAN İPEKOĞLU** under the supervision of **PROF. DR. SADETTIN ORHAN** and we certify that in our opinion it is fully adequate, in scope and in quality, as a thesis for the degree of Master of Science.

Prof. Dr. SADETTİN ORHAN

Supervisor

Assoc. Prof. Dr. BARIŞ KALAYCIOĞLU

Jury Member

Assoc. Prof. Dr. HAKAN ARSLAN

Jury Member

Prof. Dr. SADETTİN ORHAN

Director

Graduate School of Natural and Applied Sciences

ETHICAL DECLARATION

I hereby declare that, in this thesis which has been prepared in accordance with the Thesis Writing Manual of Graduate School of Natural and Applied Sciences,

- All data, information and documents are obtained in the framework of academic and ethical rules,
- All information, documents and assessments are presented in accordance with scientific ethics and morals,
- All the materials that have been utilized are fully cited and referenced,
- No change has been made on the utilized materials,
- All the works presented are original,

and in any contrary case of above statements, I accept to renounce all my legal rights.

Date: 29 November 2024 **Signature:**

Name & Surname: Furkan İPEKOĞLU

ACKNOWLEDGMENTS

Firstly, I would like to express my sincere gratitude to my supervisor, Prof. Dr. Sadettin ORHAN for their invaluable guidance and support during my thesis. His deep expertise and insightful suggestions have significantly enriched this work.

2024, November **Furkan İPEKOĞLU**

NUMERICAL INVESTIGATION OF A SLIDER CANOPY LOCKING MECHANISM

ABSTRACT

Canopy locks are the basis of flight safety. It is essential to prevent plastic deformation during flight, the expected maximum elastic deformation within acceptable limits and adjustability capabilities for different tolerance situations for canopy locking mechanisms.

In this study, four different designs of PH13-8Mo (AMS 5629) were considered. The first design, which is the fixed locking structure was compared with three different designs designed at different eccentricity levels and numerically examined.

First, a fixed and traditional pin design was modelled by using CATIA software. Then an eccentric pin design was considered to provide an adjustable solution with the same dimensions. After the design stage, to obtain displacement and stress the finite element analysis was performed using ANSYS software. In this first step, the necessary displacement and stress values could not be obtained in the structure. For this reason, some improvements at the connection points of the pin support were accomplished and a double wall housing structure was designed. After realizing that the designed double walled pin housing reduced the displacement and stress values, an extended double walled eccentric pin housing was designed by expanding the wall gaps as an alternative.

As a result of the analysis, it was observed that the highest displacement and stress values took place in the eccentric pin structure of the single-support wall . Although the fixed pin structure demonstrated better structural properties than the single support wall eccentric pin structure, it did not present as low as stress and displacement performance as the double supported pins. It was seen that the preference for double supported eccentric pin structures in similar locking mechanisms reduces the loads on the pin and pin body and reduces the expected displacement values in the structure.

Keywords: Canopy, mechanism design, eccentric pins, PH13-8Mo, finite element method, stress.

BİR KAYAR KANOPİ MEKANİZMASINA AİT KİLİT YAPISININ SAYISAL OLARAK İNCELENMESİ

ÖZ

Kanopi kilitleri uçuş güvenliği için hayati öneme sahiptir. Kanopi kilitlerinden uçuş sırasında plastik deformasyona uğramaması, elastik deformasyonunun sınırlı olması ve farklı tolerans gerektiren durumlara uygun ayarlanabilir olması beklenmektedir.

Bu çalışmada PH13-8Mo (AMS 5629) malzemeye sahip, dört farklı tasarım ele alınmıştır. Bu tasarımlarda ilki olan sabit kilit yapısı, farklı eksantriklik seviyesinde tasarlanmış üç farklı tasarım ile karşılaştırılmış ve sayısal olarak incelenmiştir.

Bu doğrultuda, öncelikle sabit ve geleneksel bir pin tasarımı CATIA yazılımı ile modellenmiştir. Ardından aynı boyutlarda ayarlanabilir bir çözüm sunmak amacıyla tasarıma eksantrik pin eklenmiştir. ANSYS yazılımı kullanılarak yapılan sonlu elemanlar analizi sonucunda yapıda istenilen deplasman ve gerilme değerleri elde edilemediği için, pini destekleyen bağlantı noktalarında iyileştirmeler yapılarak çift duvar yapısı tasarlanmıştır. Tasarlanan çift duvara sahip pin yuvasının deplasman ve gerilme değerlerini düşürdüğünün fark edilmesi üzerine, alternatif olarak duvar aralıkları genişletilerek çift duvarlı uzatılmış eksantrik pin yuvası tasarlanmıştır.

Yapılan analizler sonucunda; tek destek duvarlı eksantrik pin yapısının en yüksek deplasman ve gerilme değerlerine sahip olduğu gözlemlenmiştir. Sabit pin yapısı tek destek duvarlı eksantrik pin yapısından daha iyi yapısal özellikler gösterse de çift destekli pinler kadar düşük gerilme ve deplasman performansına sahip değildir. Çift destekli eksantrik pin yapılarının benzer kilit mekanizmalarında tercih edilmesi, pin ve pin gövdesi üzerindeki yüklerin azalmasını ve yapıda beklenen deplasman değerlerinin düşmesini sağlayacaktır.

Anahtar Kelimeler: Kanopi, mekanizma tasarımı, eksantrik pinler, PH13-8Mo, sonlu elemanlar yöntemi, gerilme.

CONTENTS

M.Sc. THESIS EXAMINATION RESULT FORM ii
ETHICAL DECLARATION iii
ACKNOWLEDGMENTS iv
ABSTRACT v
ÖZ vi
LIST OF TABLES ix
LIST OF FIGURES x

CHAPTER 1 - INTRODUCTION 1
1.1 Canopy Structure 5
1.2 Safety Issues Associated with Canopy 6
1.3 Canopy Failure due to Locking Mechanism 7
1.4 Previous Studies 10

CHAPTER 2 OVERVIEW 12
2.1 Canopy Requirements 12
2.1.1 Bird Strike 12
2.1.2 View Angle 13
2.1.3 Ejection Envelope 14
2.1.4 Loads 14
2.1.5 Airtightness and Canopy Seals 15
2.2 Design Alternatives 18
2.2.1 Forward Hinged Canopies 18
2.2.2 Rear Hinged Canopies 22
2.2.3 Sliding Canopies 24
2.2.4 Sideways Canopies 27

CHAPTER 3 - METARIALS AND METHOD 28
3.1 Material 28
3.2 Methods 32
3.3 Finite Element Analysis 37
3.3.1 Geometry Creation 38

3.3.2 Material Properties Definition 40
3.3.3 Boundary Conditions 41
3.3.4 Calculation of Effected Loads 42
3.3.5 Meshing 45
3.3.6 Pre-Processing Effects 51
3.3.7 Contact Type 53

CHAPTER 4 - RESULTS AND DISCUSSION 57
4.1 Deflection Values 57
4.2 von-Mises Stresses 60
4.3 Maximum Principal Stresses 65
4.4 Maximum Shear Stresses 69

CHAPTER 5 - CONCLUSION 74
5.1 General Conclusion 74
5.2 Recommendations for the Future Work 75

REFERENCES 76

CURRICULUM VITAE 80

LIST OF TABLES

Table 3.1 Mechanical properties of PH13-8Mo for different conditions [39]..... 30

Table 3.2 Mechanical Properties of PH13-8Mo, PH15-5 and PH17-4 [39]..... 31

Table 3.3 Table Eccentric pin dimensions 35

Table 3.4 Table Pin housing dimensions 36

Table 3.5 Mechanical properties of PH13-8Mo material [35]..... 41

Table 4.1 Average Deflection Values Based on Design 57

Table 4.2 Average von-Mises stress values based on design..... 61

Table 4.3 Maximum principal stress values based on design..... 65

Table 4.4 Maximum shear stress values based on design..... 69

LIST OF FIGURES

Figure 1.1 T-38 Transparencies [7] 2

Figure 1.2 A plane without canopy (The Royal Aircraft Factory S.E.5)..... 3

Figure 1.3 A plane without canopy but windshield..... 4

Figure 1.4 Modern canopy F-22..... 5

Figure 1.5 TAC ATTACK magazine F-4 lost canopies [11] 8

Figure 1.6 F-22 canopy failures [12]..... 9

Figure 1.7 Canopy failure due to locker mechanism, (a) fully locked and (b) partially locked [15] 10

Figure 2.1 Bird strike by impact area on airframe [23]..... 12

Figure 2.2 CPCS pressurization schedule for a typical fighter aircraft [26] 15

Figure 2.3 Demonstration and loads of inflatable seal [31] 16

Figure 2.4 Design criteria of inflatable seal for (a) outside, (b) inside and (c) axial directions [32] 17

Figure 2.5 Canopy locking mechanism cutouts on JSF F-35 longeron [33]..... 20

Figure 2.6 Rear Hinged F-16 canopy locking mechanism [34] 23

Figure 2.7 (a) The locking and (b) unlocking phase [35]..... 24

Figure 2.8 Detailed view of F-22 canopy latching mechanism [36]..... 25

Figure 2.9 (a) Pin Locations and (b) detailed view of J-20 canopy latching mechanism [37] 26

Figure 3.1 Engineering stress-strain curves of cast PH 13-8 Mo stainless steel for different aging conditions [40]. 32

Figure 3.2 Sliding Canopy Locking Mechanism Diagram 34

Figure 3.3 Demonstration of eccentric pin structure with dimensions 35

Figure 3.4 Pin housing demonstration with dimensions 36

Figure 3.5 Finite element analysis workflow 37

Figure 3.6 (a) Fixed mechanism, (b) single wall supported mechanism..... 39

Figure 3.7 (a) Double wall supported mechanism, (b) Extended double wall mechanism..... 40

Figure 3.8 Material definition on ANSYS 41

Figure 3.9 Beam elements used for bonding to ground 42

Figure 3.10 Application of the calculated force for each pin..... 45

Figure 3.11 Mesh model of double wall supported eccentric pin 46

Figure 3.12 Element Size and von-Mises stress relationship..... 47

Figure 3.13 Stress difference for each element size ……47

Figure 3.14 Stress distribution of point and pressure load..... 49

Figure 3.15 Typical sharp corner of 90º – Contour of the stress singularity and its local effect..... 50

Figure 3.16 Skewness mesh spectrum..... 50

Figure 3.17 Complex state of the solid model 52

Figure 3.18 Simplified state of the solid model 53

Figure 3.19 Master and slave bodies for no seperation contact relationship 55

Figure 4.1 Total deflection gradient for fixed pin solution 58

Figure 4.2 Total deflection gradient for single wall eccentric pin..... 58

Figure 4.3 Total deflection gradient for double wall eccentric pin 59

Figure 4.4 Total deflection gradient for extended double wall eccentric pin..... 59

Figure 4.5 Results of total deflection based on eccentricity levels 60

Figure 4.6 von-Mises stress distribution on fixed pin solution..... 62

Figure 4.7 von-Mises stress distribution on single wall eccentric pin 62

Figure 4.8 von-Mises stress distribution on double wall eccentric pin..... 63

Figure 4.9 von-Mises stress distribution on extended double wall eccentric pin 63

Figure 4.10 von-Mises stress distribution based on eccentricity levels for pin structure..... 64

Figure 4.11 von-Mises stress distribution based on eccentricity levels for housing structure..... 64

Figure 4.12 von-Mises stress distribution for (a) linear pin structure and (b) maximum eccentric pin, double wall extended housing structures 65

Figure 4.13 Maximum principal stress distribution on fixed pin solution 66

Figure 4.14 Maximum principal stress distribution on single wall eccentric pin 66

Figure 4.15 Maximum principal stress distribution on double wall eccentric pin 67

Figure 4.16 Maximum principal stress distribution on extended double wall eccentric pin 67

Figure 4.17 Maximum principal stress distribution based on eccentricity levels for pin structure 68

Figure 4.18 Maximum principal stress distribution based on eccentricity levels for housing structure 69

Figure 4.19 Maximum shear stress distribution on fixed pin solution 70

Figure 4.20 Maximum shear stress distribution on single wall eccentric pin 70

Figure 4.21 Maximum shear stress distribution on double wall eccentric pin 71

Figure 4.22 Maximum shear stress distribution on extended double wall eccentric pin 71

Figure 4.23 Maximum shear stress distribution based on eccentricity levels for pin structure 72

Figure 4.24 Maximum shear stress distribution based on eccentricity levels for housing structure 72

CHAPTER 1

INTRODUCTION

Throughout history, people have always had a passion for flying and soaring through the skies. The Ancient Greek philosopher Aulus Gellius was designed and the first self-propelled flying device around 400 BC. The machine was flown 200 meters[1]. Although it is well known that Hezarfen Ahmed Çelebi, who lived in the early 1600s, flew from the Galata Tower to the Bosphorus with the help of the southwestern wind, known as first flew human by manned rocket [2], Ibn Firnas, who lived in the 9th century, had first flight attempts [3]. American Wright Brothers, Orville and Wilbur Wright, invented the first motorized airplane in 1903 [4].

Canopy is the one of the most important component that directly ensures flight safety. First, it must provide minimum air leakage while climbing high altitudes, clear vision of the surroundings and high impact resistance against foreign objects, such as birds [5]. This protection plays a pivotal role in flight safety and crew team comfort.

Canopy structure shall be a single part or combination of different transparencies such as windshield, forward canopy and aft canopy. Figure 1.1 shows tandem combination for T-38 aircraft. However, single piece canopy also shall be made from lamination of different materials such as polycarbonate and acrylic to prevent damage any case of bird strike and ejection envelope path in case of emergency situations at the same time [6].

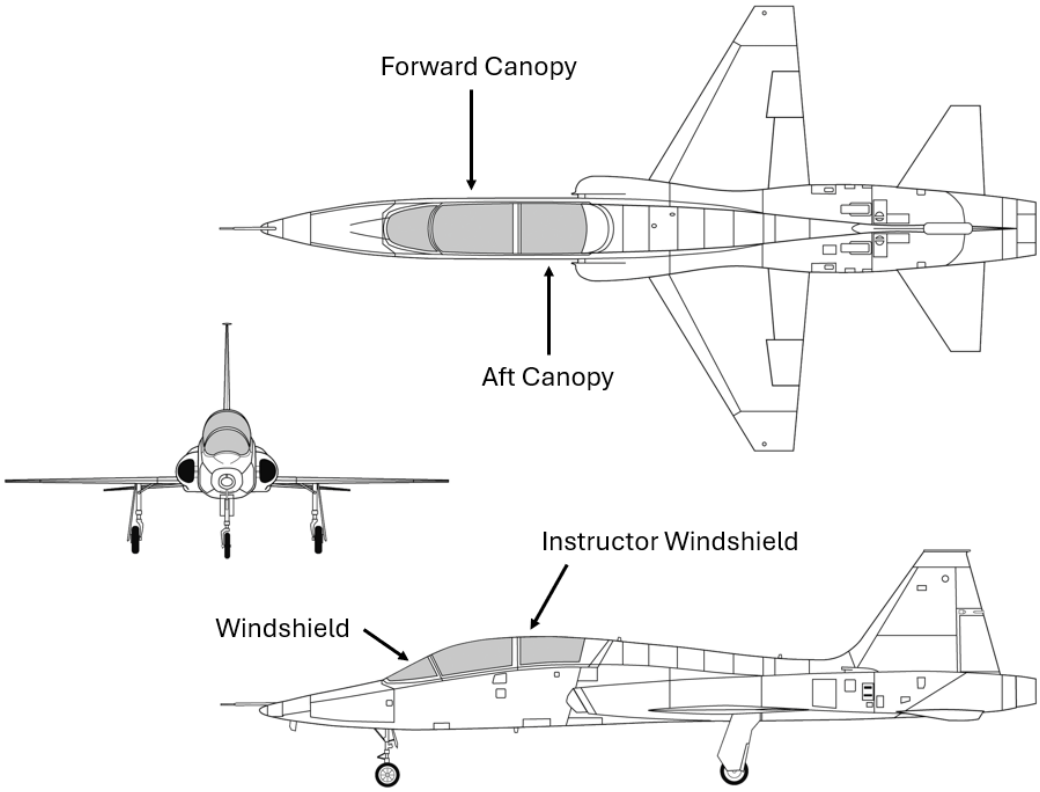

Figure 1.1 T-38 Transparencies [7]

The development of aircraft canopies reflects the evolution of aviation technology and pilot safety. At the beginning of the invention of aircrafts have no canopies. They have only open cockpits. An example of this is shown in Figure 1.2. These early designs were functional for the low speeds and short distances. However, lack of the performance this type of aircraft did not prioritize cockpit protection. Therefore, pilots were face to face with the air flow, birds strike and atmospheric conditions. However, pilot safety gone emphases by the late 1910s, leading to the introduction of basic canopy designs. These early canopies were primarily made of flat glass panels, which provided minimal protection against wind and rain but were a significant advancement over completely open cockpit.

Figure 1.2 A plane without canopy (The Royal Aircraft Factory S.E.5)

During the 1920s and World War II, as aviation technology advanced, fully enclosed cockpits became necessary due to the increasing speeds and altitudes of aircraft. Improved aerodynamic performance and pilot protection requirements led to the switch to new canopies. Early canopies were often framed by several sheets of glass. Although these of canopies offering some protection, also made it difficult to see outside because of the supports. During this time, acrylic materials were introduced, which was a major improvement [8].

Acrylic canopies were lighter, more flexible and less prone to breakage than traditional glass, allowing for more innovative designs that increase visibility and reduce drag [9].

A transparent enclosure covering the cockpit of certain aircraft models is called an aircraft canopy. Over a conventional flight deck, an aircraft canopy offers much wider vision while also providing a controlled and pressurized cabin atmosphere for the crew team. An aerodynamic canopy's shape is a compromise that maximizes vision for pilots and other crew members while minimizing aerodynamic drag.

Although most flights took place in favourable weather, early aircraft were not designed with canopies, leaving pilots exposed to the elements. Most aircraft lacked canopies even during World War I, yet tiny windshields were sometimes employed to shelter pilots from wind and propeller wash like in Figure 1.3. A fully enclosed cockpit with a canopy grew more and more popular as airplanes gained speed and altitude in the 1920s and 1930s [10].

Figure 1.3 A plane without canopy but windshield

Early aircraft canopies were made from several flat glass panels held together by frames and muntin's, which obstructed visibility an issue particularly troublesome for military pilots. These glass canopies were also heavier than the acrylic ones that began to be used just before World War II. As advancements in aviation technology, aircraft design and manufacturing methods progressed, the need for improved canopies became faster and evident. This led to the introduction of the more aerodynamic acrylic bubble canopy, which greatly improved pilot visibility and operational efficiency.

During and after World War II, the bubble canopy design emerged as a solution to visibility problems. It provided pilots with a 360-degree view and became a standard feature on many fighter aircraft [11].

The development of unbreakable laminated safety glass and clear plastics played a major role in the evolution of canopies. These materials allowed for the creation of more fluid and safer cockpit enclosures, meeting the demands of higher speeds and altitudes.

By the late 1930s, enclosed cockpits became commonplace, greatly improving pilot comfort and safety. Advances in materials science, particularly the co-evolution of plastics and cockpit design, played a major role in shaping the modern aircraft canopy. The F-22 in Figure 1.4 has an advanced modern canopy.

The importance of air dominance in national defense is on the rise. This can only be achieved with an air force equipped with advanced fighter jets that offer enhanced maneuverability, along with highly skilled personnel.

Figure 1.4 Modern canopy F-22

1.1 Canopy Structure

A canopy structure can be fundamentally composed of several key components, including the canopy frames, locking mechanism, transparency and sealing gaskets, all of which work together to ensure the integrity and functionality of the overall assembly.

The most significant load that a canopy is subjected to is the cabin pressure within the cockpit. The canopy glass is responsible for transferring this internal pressure to the canopy frames. These frames then distribute the load to the aircraft's fuselage, utilizing locking mechanisms to ensure the pressure is effectively managed and contained.

According to MIL-C-81590, manual actuation of canopies is generally impractical for those weighing over 80 pounds (approximately 36 kg). To mitigate this challenge, counter-balance devices should be incorporated to ensure that the force required to move the canopy does not exceed 20 pounds (approximately 9 kg). When designing canopies that utilize manual actuation, it is essential to ensure that the canopy can be operated through its entire range of motion by any crew member while they are positioned in their normal flight seat. Although inertia reels and other emergency devices can be considered "unlocked" during routine flight operations, it is crucial that all straps, belts and securing mechanisms are correctly installed and firmly secured to maintain safety and functionality [12].

1.2 Safety Issues Associated with Canopy

There are several reasons to canopy failures.

Mechanical Failure: One of the main mechanical problems is related about functionality of the canopy. Canopy may not open when closed or may not close when opened. These kinds of problems may result of multifunction of hydraulic or electrical systems. However, broken latches, faulty actuators or seals which stucked between canopy and fuselage may lead to failure of the canopy.

Structural Failure: The canopy may have structural problems such as cracks or spalling. This could compromise the pilot's vision and protection. In some severe cases, the canopy may break away from the aircraft.

Sealing Issues: Canopies are designed to be airtight to protect the cockpit from the elements and to maintain pressurization. Pressurization issues in the cockpit, water intrusion or debris entering the cockpit can result from improper sealing.

Material Fatigue: Repeated stress and inadequate bonding within the canopy

structure can lead to fatigue cracks. These may result a catastrophic failure of canopy.

Environmental Factors: Extreme temperature changes, exposure to chemicals and physical impacts can deteriorate the canopy material and cause failures.

Visibility Issues: Problems with the transparency of the canopy, such as fogging, scratching or deterioration of the material, can obstruct the pilot's vision. Visibility Issue is vital for safe flight and pilot safety.

Ejection System Failures: Canopy is often part of the ejection system in fighter jets and some other aircraft. If the canopy does not separate properly during an emergency ejection, it can seriously endanger the pilot's safety.

Canopy failures can be serious and potentially life-threatening. For these and similar reasons, aircraft are designed with multiple safety systems and maintenance protocols to address and prevent these problems [13]. Regular inspections and maintenance are essential to ensure the canopy remains in good working condition [13].

Due to these reasons, canopy is one of the crucial component of aircraft and pilot life. This thesis examines strategies to prevent mechanical and structural failures in canopies. Furthermore, it proposes a designed canopy locking system intended to mitigate other potential failures and issues that may occur in canopies.

1.3 Canopy Failure due to Locking Mechanism

In 1972, the article written by US Air Force soldiers and published in TAC ATTACK magazine criticized the condition of F-4 Phantom jet fighter which lost its canopy. US Air Force authorities says the Canopy losses have plagued the Phantom since it first rolled off the assembly line. The report says "Besides being dangerous, this gets expensive - especially when we she out approximately $6,000 per canopy". Then the report emphasizes that the main reason of is stalled canopies %62 and shear pin failure %7 which are mechanical locker systems [14]. Cover page of the TAC ATTACK magazine can be seen in Figure 1.5.

Figure 1.5 TAC ATTACK magazine F-4 lost canopies [11]

When it is considered the recent plane crashes, it is seen that the canopy system plays an important role. According to US 1st Maintenance Group report, F-22 pilot was locked inside the cockpit of his aircraft for five hours. The report says "-On 10 April 2006 at approximately 0815 aircraft 03-041 had a Red Ball for a canopy unlock indication. Attempts to clear the problems by cycling the canopy failed. The final cycling of the canopy resulted in its the down and locked position. The canopy would not cycle up form this position trapping the pilot in the cockpit. The aircraft subsequently ground aborted. Attempts to manually open the canopy were unsuccessful-". In addition, the canopy replacement cost is $182,205 and total damage to the airplane is $1.28 million [15]. Figure 1.6 shows the broken canopy of F-22.

Figure 1.6 F-22 canopy failures [12]

In 2020, USAF Technical Airworthiness Authority (TAA) imposed an altitude restriction of 35000 feet and no cabin pressurization on the fleet of jet fighters. The objective of the ESi investigation was to identify the failure mechanism, cause of failure and preventive actions. The report says "time-delayed failure mechanisms (i.e., material degradation, environmental stress cracking and/or fatigue) was absent" due to mechanical parts [16].

On April 2, 2022, the canopy of an Extra NG aircraft broke apart during straight and level flight. On April 2, 2022, the canopy of an Extra NG aircraft broke apart during straight and level flight. The British [17] and Poland State Commission on Aircraft Accidents Investigation [18] authorities say that "After accelerating up to 350 kph and levelling the flight, the canopy suddenly opened, broke and part of it detached from the aircraft". The pilot sustained serious injuries and had to bail out as the aircraft entered a descent and collided with a building. The investigation revealed inadequate bonding between the inner and outer canopy frame, leading to fatigue crack

development and eventual catastrophic failure. Figure 1.7 shows the locking mechanism which leads to failure. Fully locked and partially locked statutes can be seen in Figure 1.7 (a) and Figure 1.7 (b) respectively.

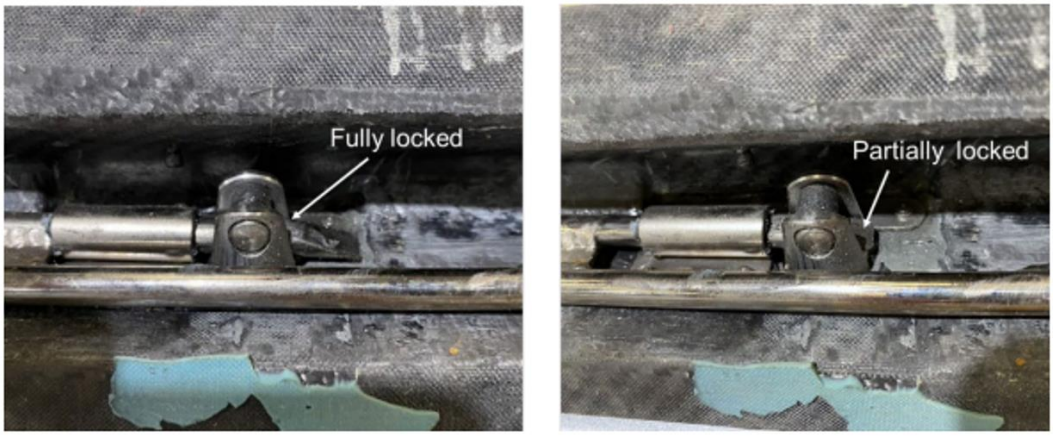

Figure 1.7 Canopy failure due to locker mechanism, (a) fully locked and (b) partially locked [15]

1.4 Previous Studies

There are papers with limited number regarding the topic. It is believed that since the topic is related to defense, scientists do not want to publish their findings due to security issue. Previous studies published related the topic are presented in below.

In 1957, Cowan had suggested an invention for locking and actuating mechanism for aircraft cockpits. The mechanism described operates the canopy of an aircraft, allowing it to be opened and closed in a specific sequence while managing the locking latches and inflatable seal. It utilizes solenoids to control hydraulic valves, enabling operation from both inside the cockpit and externally. The system includes mechanical linkages connecting locking levers to ensure coordinated movement and functionality [19].

George H. Nichols has developed an aircraft canopy locking mechanisms [20]. The canopy lock is a device used to secure the transparent enclosure that covers the cockpit of an aircraft. The invention provides a safe and improved canopy lock for aircraft canopies, specifically clamshell types, that is practical, economical and reliable. It

features a pair of dogs mounted in the cockpit, a handle for manual actuation from both inside and outside and a spring-loaded pin-and-detent retainer for positive locking capabilities. This design allows for easy operation and secure locking, even under emergency conditions.

The paper written by Shen et al. investigates the failure analysis of a lock mechanism and the degradation of its components. It employs a two-phase degradation model and Vine Copula to analyse the time-varying dependence between the degradation processes. The findings highlight the importance of accurately modelling component reliability and their contributions to overall system failure [21].

At Poland Military Institute of Engineer Technology, Jasiński et al. focused on design and dynamic analysis of a backlash-free locking mechanism for sliders. The paper presents a design and dynamic analysis of a backlash-free locking mechanism for a slider, which compensates for inaccuracies and wear within a ±1.5 mm range. The study highlights the advantages of using dynamic simulations to reduce the need for costly physical tests during the design process. On the other hand, even slider connected to a movable element high weighing, suggested work is not suitable for aircraft canopy system [22].

CHAPTER 2

OVERVIEW

2.1 Canopy Requirements

The designed canopy must ensure both safety and functionality of the crew in terms of various aspects. The primary considerations for achieving this can be listed as follows:

2.1.1 Bird Strike

JSSG-2006 reports that 20.4% (which is significantly high percentage for whole fuselage components) of the bird strikes occur on the canopy. However, only seven percent of these resulted in shattered transparencies. The other category includes bird strikes on the landing gear, vertical and horizontal stabilizers, flaps, fuselage, and ordnance. The impact area on fuselage of birds can be seen in Figure 2.1, [23].

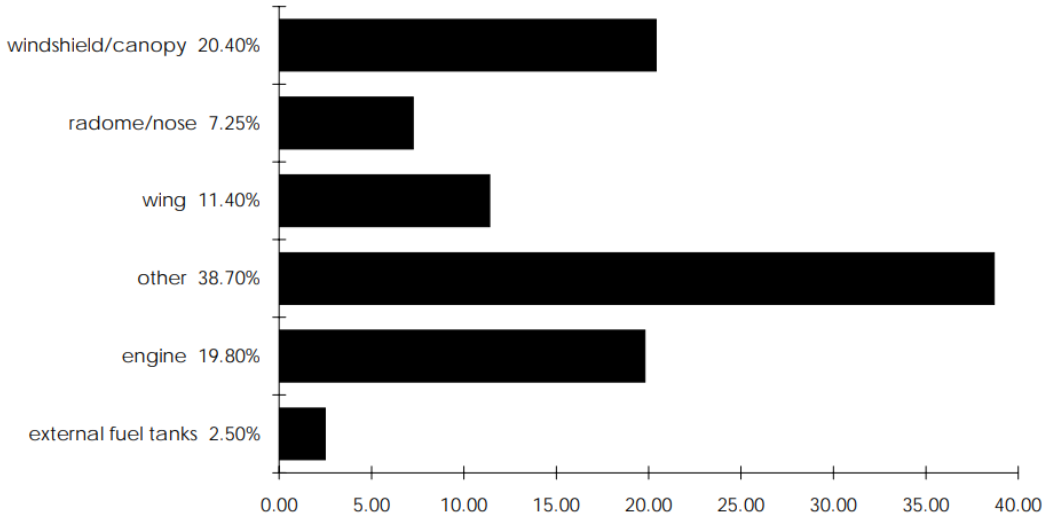

Figure 2.1 Bird strike by impact area on airframe [23]

In accordance with CS 25.631, aircraft are required to be designed to endure the impact of a 4 lb bird while maintaining safe flight and landing capabilities. The regulation specifies that the critical velocity at which this bird strike must be accounted for is determined by comparing two different velocity conditions. Firstly, the aircraft's

velocity at sea level, designated as VC, must be considered. VC is known as design cruse speed for aircraft. Secondly, the critical velocity is also defined as 0.85 times VC at an altitude of 2438 meters (8000 feet). The more stringent of these two velocities whichever is higher becomes the standard for the design requirement [24].

To comply with this regulation, aircraft manufacturers must ensure that their designs are robust enough to withstand a bird strike at this maximum critical velocity. This involves rigorous testing and structural reinforcement to guarantee that the aircraft can continue to operate safely and perform a successful landing even after sustaining damage from a collision with a bird of this size under the specified conditions.

2.1.2 View Angle

The reference plane used to define vision angles is the pilot's horizontal line of sight, measured relative to the aircraft's longitudinal fuselage reference line. The zero azimuth reference is established as the line directly aligned with the designated eye position.

According to MIL-STD-850, to ensure flight safety, the canopy structure must be sufficiently wide to provide the mission crew with specific angles in various directions. These angles are listed below [9].

1. At 0° azimuth, at least 11° down and 10° up

2. At 20° azimuth, Left and right, 20° down.

3. At 30° azimuth, left and right, 20° down

4. At 90° azimuth, left and right, 40° down.

5. At 135° azimuth, left and right, 20° down

To provide such extensive viewing angles, a canopy must feature a wide surface area. However, this increased surface area also means that the canopy is subjected to higher cabin pressure. Consequently, the larger pressure load results in greater forces being exerted on the canopy structure. This additional stress not only affects the structural

integrity of the canopy itself but also places increased demands on the locking mechanisms, which must accommodate and manage these greater forces effectively to maintain safety and functionality.

2.1.3 Ejection Envelope

A significant level of threat is inherent in several facets of military aviation due to the potential for enemy action or loss of control during aggressive low-altitude manoeuvres. Because of this, most training and combat aircraft are standard equipped with a form of mechanism designed to help with crew escape [25].

The pilot should be able to use the ejection seat to exit the aircraft in the case of a negative situation. The canopy, also known as the transparency, must be designed to either break (canopy fracture) or lift away from the aircraft's fuselage together with its supporting frames (canopy jettison), in order to guarantee the pilot’s ejection path.

To guarantee the without limitation escape of the pilot, the ejection seat system should make it easier to remove the canopy or its frames. This design requirement is essential to enable the pilot to depart from the aircraft safely and quickly in an emergency, acting as a vital safety precaution to preserve the pilot's life.

Furthermore, the canopy locks must be robust and reliable to ensure proper functionality in these situations. Effective management of the canopy's separation is crucial for a successful ejection and the durability of the canopy locks is essential for facilitating this process.

2.1.4 Loads

The load that an airplane encounters when moving on the ground, such as landing or towing, is referred to as a ground load. However, air pressure applied to the structure while in flight due to the manoeuvres of the aircraft.

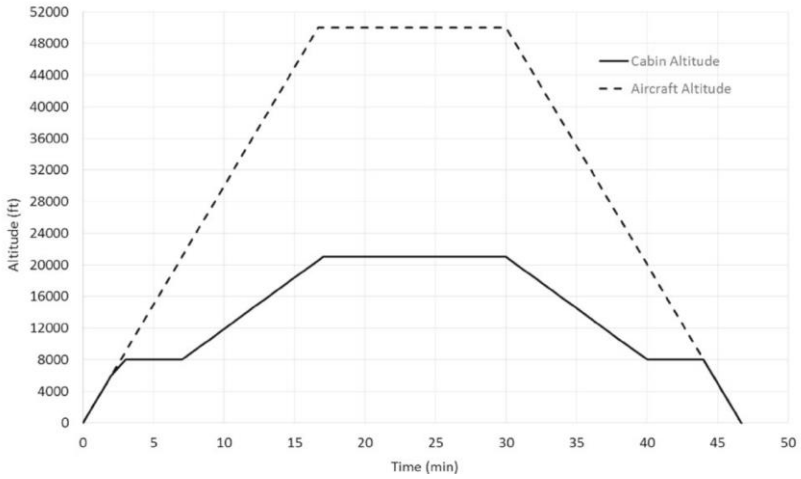

Figure 2.2 CPCS pressurization schedule for a typical fighter aircraft [26]

Although the cabin pressure is adjusted to remain at a certain level, it is noted that for fighter aircraft, the cabin pressure increases with the increasing acceleration. CPCS system work principle and pressure difference can be seen in Figure 2.2 [26].

There is no pressure difference between cabin and atmospheric pressure while climbing from sea level to 8000 ft. However, after 8000 ft, cabin pressure control system works at 5psi differential pressure between the cabin and outer pressures (approximately 21000 ft) [27].

It is known ceiling altitude of F/A-18 Hornet is 50000 ft. Any other jet may increase this 5 psi pressure difference for higher altitudes. In this study, this 5 psi differential limit exceeded for 55000 ft altitude [28].

2.1.5 Airtightness and Canopy Seals

Every machined part produces a tolerance gap [29]. Thus, pressurized cockpits must be airtight in accordance with the specifications outlined in MIL-P-18927 when the aircraft is in flight or when the engines are running. Seals at the interface between the canopy and the primary structure should be designed to minimize leakage, excessive closing forces and sliding friction.

The use of self-pressurizing seals should be evaluated as they can enhance sealing performance. The seal material must be resistant to adverse changes in its properties

when exposed to both the flight and ground environments. To prevent damage during entry and exit from the cockpit, seals should be installed on the canopy rather than on the underlying structures.

The inflatable seal grows or increases in height as the gap between the cockpit and the canopy increases and when deflated the seal retract from the structure. Aircraft designers can solve many sealing problems with this type of seal, especially those where gap variations or growth are caused by pressure, thermal, or mechanical movement. This type of seal has the unique ability to move with structural deflections when inflated and then to retract from structure contact upon deflation. Inflatable seal working principle and external forces can be seen in Figure 2.3 [30].

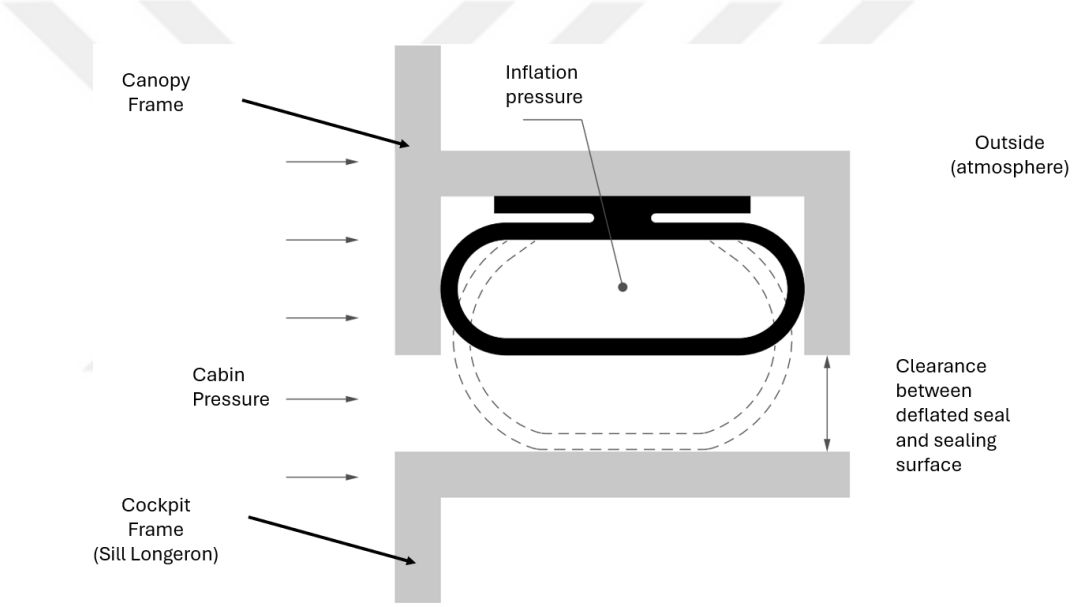

Figure 2.3 Demonstration and loads of inflatable seal [31]

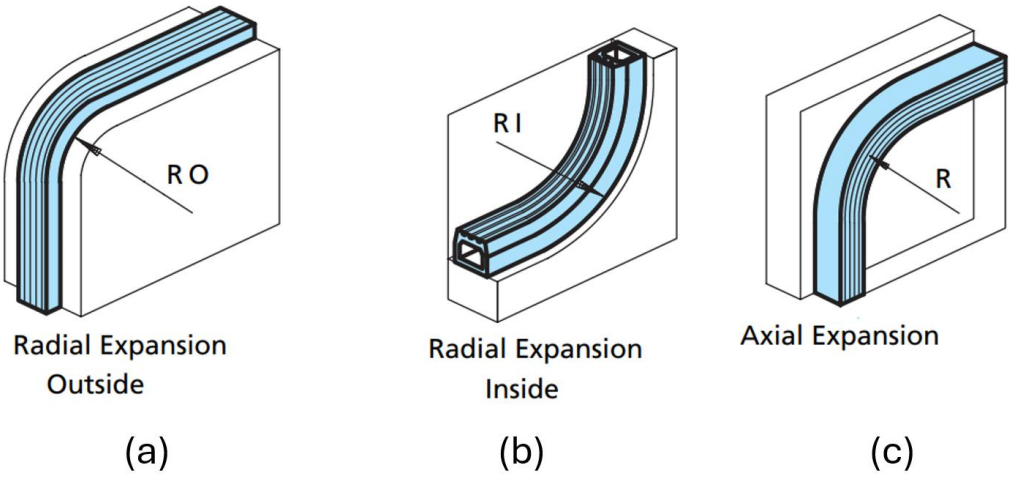

Figure 2.4 Design criteria of inflatable seal for (a) outside, (b) inside and (c) axial directions [32]

However, the maximum height that can be inflated is strictly limited by the design features of canopy, which are affected by factors such as axial or radial expansion of the canopy frames. Figure 2.4 shows the design criteria elements for an inflatable seal. Axial expansion and radial expansion for outside and inside turns can be seen in Figure 2.4. The capacity of the canopy to expand under pressure is determined by the inflated height and specific expansion radius of each seal profile. The actual and useable values for a canopy structure are normally significantly smaller, commonly lying within the range of 8-10 mm, even though the theoretical expansion radius can range from as low as 3 mm to as much as 35 mm [32].

This restriction results from the need to balance pressure resistance, structural integrity and operational efficiency during the canopy construction. These parameters are primarily determined by the expansion properties of the canopy frames which include the materials and mechanical layout of the seal profiles. Larger expansion radii might be possible in theory, but practicality is occasionally limited by issues with manufacturing tolerances, structural stability and performance requirements. As a result, the design parameters are refined to guarantee that the canopy operates efficiently within a realistic range of 8-10 mm, offering the best possible compromise between operational dependability and expansion potential.

Therefore, it is important to select the expansion radius and inflated height carefully

in order to ensure that the canopy functions well in various scenarios while preserving its structural and functional stability.

2.2 Design Alternatives

Aircraft canopies are meticulously engineered with a range of opening mechanisms, each tailored to meet specific operational requirements and accommodate diverse cockpit configurations. These mechanisms are essential for optimizing pilot access, visibility and overall cockpit functionality. The primary canopy opening methods can be broadly categorized as follows:

2.2.1 Forward Hinged Canopies

This type of canopy pivots from the front edge, opening upward and forward. The forward-hinged design facilitates ease of pilot ingress and egress, particularly in compact or enclosed cockpit environments. This configuration is commonly utilized in fighter aircraft and high-performance jets, where rapid and efficient access is crucial. The forward-hinged canopy ensures minimal obstruction of the pilot's forward view while maintaining a streamlined profile when closed.

In the forward-opening canopy design of the F-35 aircraft, the locking mechanism is meticulously integrated into the canopy structure, while the associated locking components are strategically positioned beneath the sill longeron within the cockpit. This design approach ensures that the locking mechanism's fixed components are mounted directly on the canopy. By utilizing lighter fixed locks that are directly affixed to the canopy, the design effectively reduces the weight of the moving structure.

This reduction in weight is achieved because the lighter fixed locks decrease the overall load that the moving parts must bear. Consequently, this results in a more streamlined and efficient canopy design. The decrease in weight not only enhances the manoeuvrability and responsiveness of the canopy but also contributes to a more rigid and stable structure. The overall effect is a canopy system that benefits from improved performance characteristics, such as reduced aerodynamic drag and increased operational reliability. This design choice ultimately supports the F-35’s advanced capabilities and operational effectiveness.

In this design, specific cutouts have been made on the sill longeron to facilitate the integration of the canopy locking mechanisms within the cockpit, allowing the locking components to be positioned beneath the longeron. This adaptation was required to ensure that the locking mechanisms are effectively accommodated while maintaining the functionality of the canopy system.

However, research has demonstrated that introducing holes or cutouts that disrupt the surface continuity of structural components has a direct and significant impact on the structural integrity of the assembly. The creation of these openings leads to the development of stress concentrations around the edges of the cutouts. These stress concentrations can result in localized areas of elevated stress, which are known to adversely affect the component's overall strength and durability.

Moreover, the presence of such cutouts compromises the fatigue resistance of the structure. The stress intensities around the interruptions can accelerate the onset of material fatigue, leading to a reduced fatigue life of the structural components. Consequently, this results in a higher likelihood of premature failure under cyclic loading conditions, thereby diminishing the long-term reliability and performance of the canopy system.

Therefore, while the cutouts facilitate the necessary integration of the locking mechanisms, they also necessitate careful consideration of their impact on the structural performance.

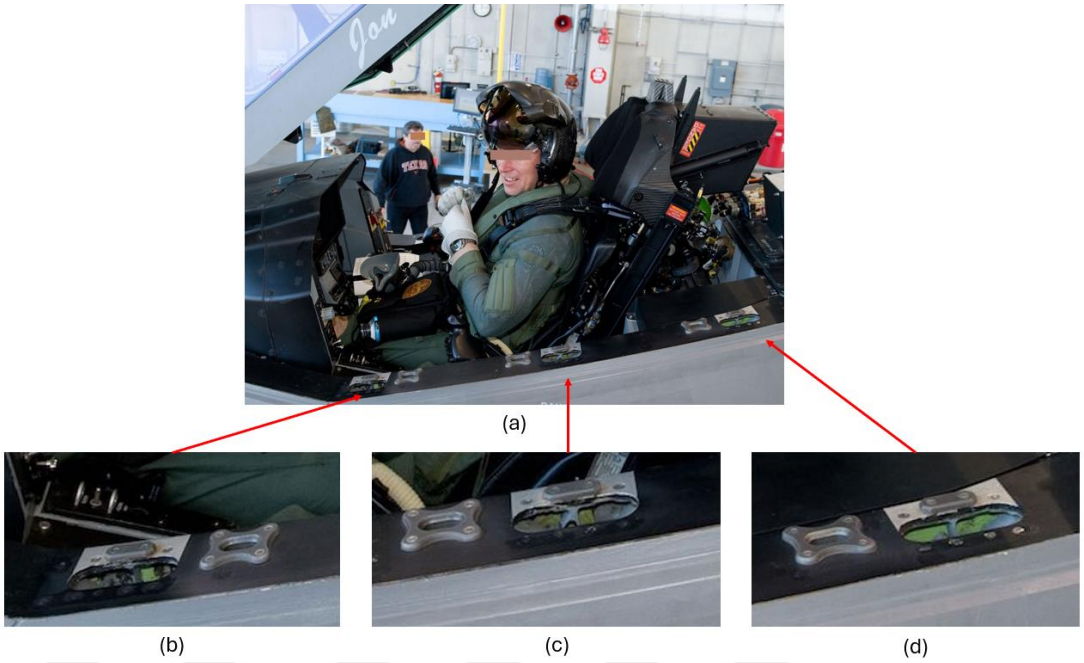

Figure 2.5 Canopy locking mechanism cutouts on JSF F-35 longeron [33]

The sill longeron is a fundamental structural component of the aircraft fuselage, playing a vital role in maintaining the integrity and strength of the overall structure. Positioned between the forward and aft pressure bulkheads, the sill longeron functions as a critical bridging element that connects these two key structural components. By linking the forward and aft bulkheads, it effectively creates a continuous structural framework that contributes to the overall stability and rigidity of the fuselage. JSF F-35 sill longeron, locking mechanism and guide pin cutouts can be seen in Figure 2.5. For this solution, front guide pin cutouts (relatively smaller cutouts) located right side of the locking cutouts, can be seen in Figure 2.5 (b). However, the second and third guide pin cutouts located on the left side of the locking cutouts, can also be seen in Figure 2.6 (c) and (d) respectively.

In addition to its role in connecting the pressure bulkheads, the sill longeron is an integral part of the pressurized cockpit wall. It provides essential support and reinforcement, helping to ensure that the cockpit maintains its structural integrity under varying pressure conditions. This is particularly important for ensuring the safety and durability of the cockpit, which must withstand significant pressures during flight.

The sill longeron also serves as the main structural element to which the cockpit frames are attached. This connection is crucial for maintaining the alignment and strength of the cockpit structure, which in turn supports the fuselage's overall robustness. By anchoring the cockpit frames to the sill longeron, the component helps to preserve the fuselage's structural continuity and integrity, which are essential for the aircraft's overall performance and safety.

Any issues with the sill longeron can lead to significant disruptions in the aircraft's maintenance schedule. Specifically, if problems arise with the sill longeron, it may necessitate the removal of both the forward and aft pressure bulkhead components, as well as other associated elements that are connected to these bulkheads. The process of addressing such issues typically requires extensive disassembly and reassembly work, which can result in the aircraft being out of service for an extended period. Consequently, this can lead to increased downtime and operational delays, impacting the overall availability and readiness of the aircraft.

Indeed, a significant issue arose with the F-15 aircraft involving the sill longeron, a crucial structural component. In this particular case, a sill longeron with an unexpectedly reduced fatigue life, due to a combination of factors, failed during flight. This failure was catastrophic, leading to the crash of the F-15C aircraft, serial number 80-0034. The failure of this component was directly responsible for the loss of the aircraft.

Following this incident, a comprehensive series of inspections were conducted across the fleet. These inspections revealed that similar issues were present in nine additional aircraft, where cracks were detected in the sill longeron components. The discovery of these cracks highlighted the systemic nature of the problem and raised serious concerns about the structural integrity of the affected aircraft.

As a result, the identified aircraft were promptly withdrawn from service for detailed maintenance and repair. This process involved extensive disassembly and thorough examination to address the cracks and prevent further failures. The necessary repairs and preventive measures were implemented to ensure that the sill longeron components met the required safety standards and to restore the aircraft to a fully

operational status.

This incident underscored the critical importance of monitoring and maintaining the structural integrity of key components such as the sill longeron. It also emphasized the need for rigorous inspection protocols and proactive maintenance strategies to detect and address potential issues before they lead to catastrophic failures. The lessons learned from this event have contributed to improved safety measures and maintenance practices to prevent similar occurrences in the future.

2.2.2 Rear Hinged Canopies

Also known as rearward-opening canopies, these pivot from the rear edge and swing backward to open. The rear-hinged design is favoured for its ability to provide a larger, unobstructed entry space and to minimize interference with the pilot's forward visibility. This design is often implemented in aircraft where maintaining a clear sightline is essential and where the rearward opening does not obstruct operational functionality.

For example, the F-16 canopy system is equipped with a rearward-opening tilt-up canopy. This design approach eliminates the need for additional space to accommodate canopy locks by integrating the locking mechanism directly within the canopy frames. As a result, this innovative arrangement not only streamlines the overall design but also significantly enhances the pilot's field of vision. By embedding the locking mechanism into the frames, the system avoids obstructing the cockpit view and ensures a more unobstructed visual perspective for the pilot. This design consideration is crucial for maintaining situational awareness and operational effectiveness during flight.

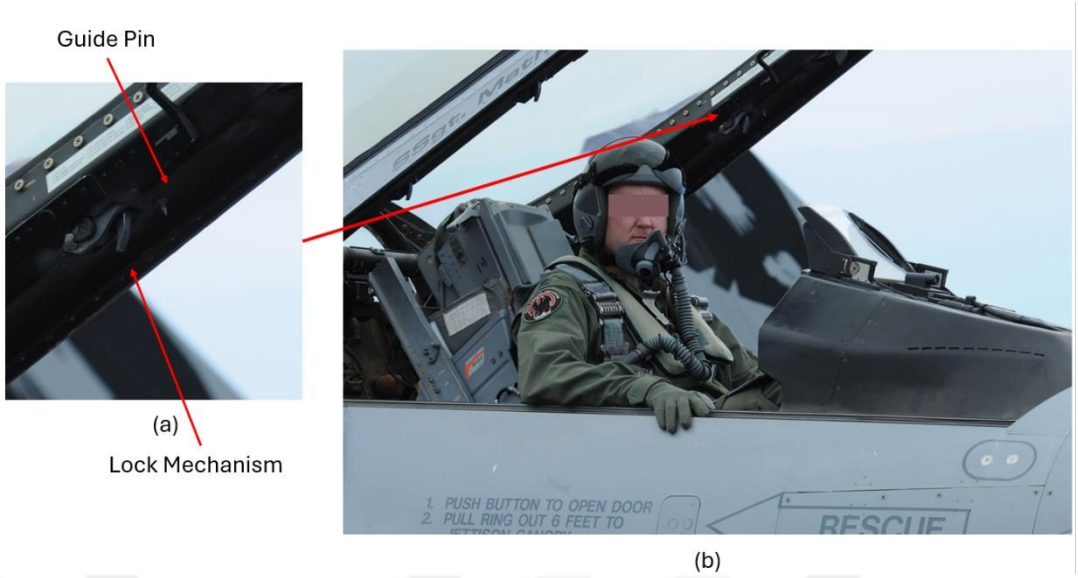

Figure 2.6 Rear Hinged F-16 canopy locking mechanism [34]

As a result of this design, the canopy structure, which is notably heavy and controlled by an actuator, has been significantly reinforced, leading to the necessity for a more robust actuator and enhanced bearing support. The integration of the locking mechanism within the canopy frames, while improving the pilot's field of vision, has increased the overall weight of the canopy assembly. This added weight places greater stress on the support bearings, which must now accommodate higher loads and thus require stronger, more durable bearing systems to ensure reliable performance. Figure 2.6 (b) is an example for a rear hinged tilt up canopy locking mechanism. Detailed view of the locking mechanism and guide pin structure can be seen in Figure 2.6 (a).

The heavier canopy not only demands a more powerful actuator to manage its movement effectively but also affects the stability of the canopy during operation. The increased load on the bearings can lead to greater wear and potential instability, making the canopy more susceptible to oscillations or yawing during movement. This instability could impact the precision and smoothness of the canopy’s operation, potentially affecting the ease and reliability of the canopy’s opening and closing mechanisms. Additionally, the increased weight and stress on the actuator and bearings may complicate the automatic locking process, potentially impeding the seamless engagement of the locking mechanism and affecting the overall safety and

functionality of the canopy system. Common locking mechanisms for hinged canopies can be seen in Figure 2.7 with in locking (a) and unlocking (b) movement.

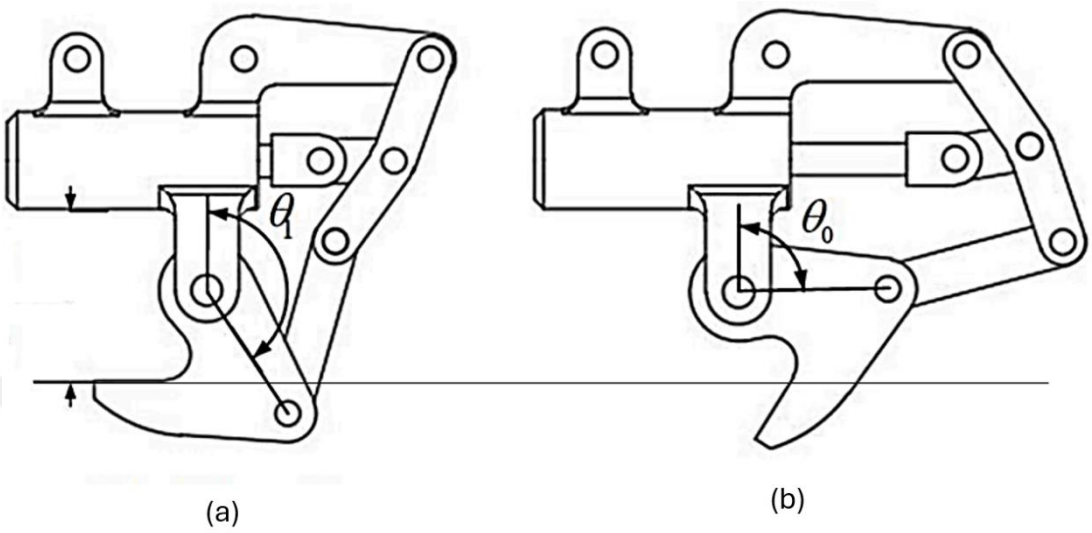

Figure 2.7 (a) The locking and (b) unlocking phase [35]

2.2.3 Sliding Canopies

Sliding canopies operate by moving horizontally, either sideways or along a dedicated track, to achieve an open position. This mechanism offers several advantages, including the ability to provide an unobstructed view when the canopy is open and a streamlined design that minimizes aerodynamic drag. Sliding canopies are particularly useful in aircraft with tight spatial constraints or where a forward or rearward-hinged mechanism would be impractical. The sliding mechanism allows for smooth and efficient access without requiring significant canopy movement.

The F-22 and J-20 aircraft, both featuring sliding canopies, are designed with a rearward-sliding and opening mechanism. One of the primary advantages of having a sliding canopy is the elimination of the need for additional locking mechanisms within the canopy or cockpit. This design choice removes the necessity for extra components that would otherwise guide the canopy during closure and bear lateral loads. Instead, the sliding canopy design relies on a cylindrical locking mechanism that not only facilitates the canopy's movement but also effectively manages lateral loads.

This streamlined design approach reduces complexity by minimizing the number of additional parts required for operation, leading to a more efficient and straightforward canopy system. By avoiding the inclusion of extra elements that would need to handle the guidance and lateral loads, the sliding canopy contributes to a lighter and more reliable overall design.

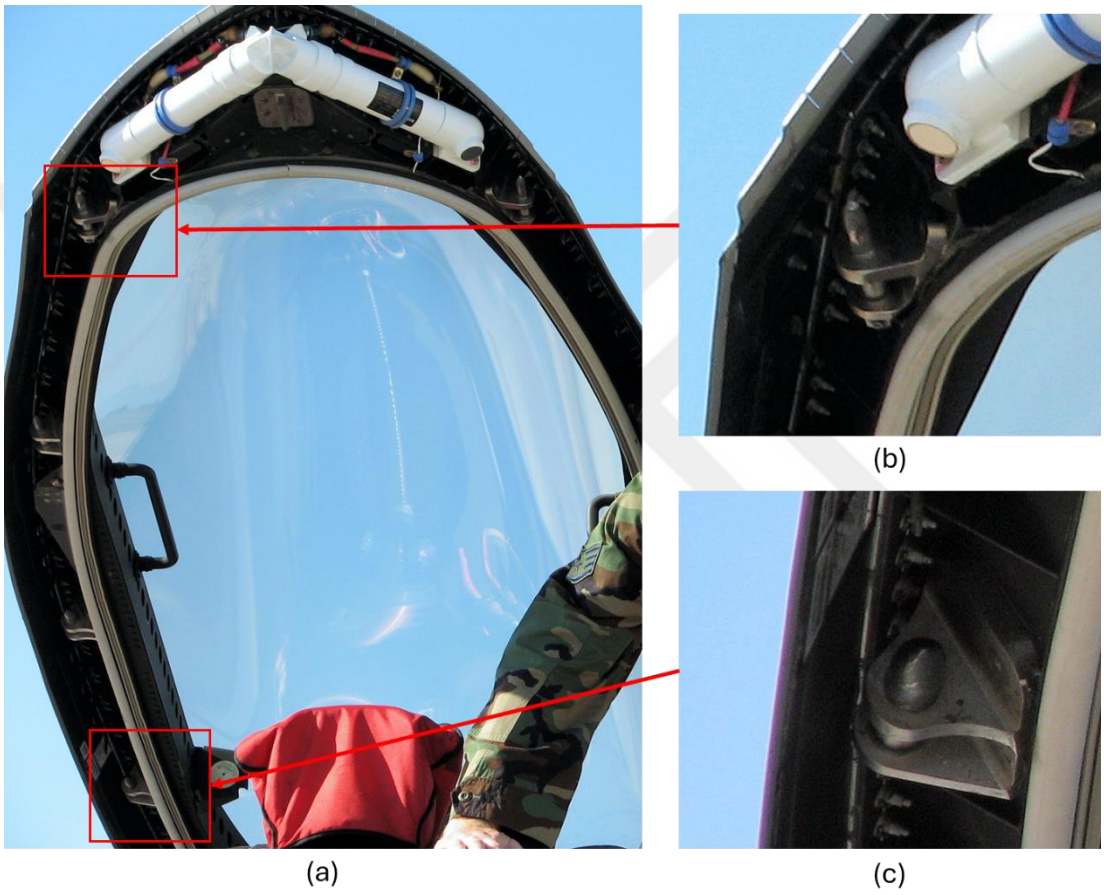

Figure 2.8 Detailed view of F-22 canopy latching mechanism [36]

As depicted in the Figure 2.8 (a), the sliding canopy is equipped with two support elements for the locking pins, each featuring a stabilizing connector located at the rear. A close view for different latching designs can be seen in Figure 2.8 (b) and Figure 2.8 (c) for front and rear respectively.

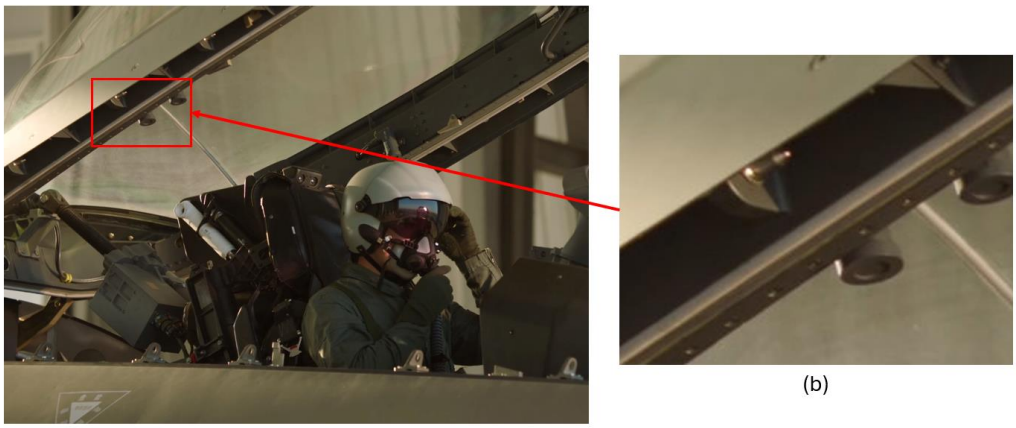

Figure 2.9 (a) Pin Locations and (b) detailed view of J-20 canopy latching mechanism [37]

In the J-20 canopy design, the locking mechanism's engagement is achieved through the movement of the canopy itself and it features a single-support pin structure. Figure 2.9 shows a detailed view of the J-20 canopy latching mechanism. This design allows for the selection of appropriate pins based on the level of eccentricity they will experience, enabling an interchangeable design approach. By adjusting the level of eccentricity between the front and rear axles of the pins, a more cost-effective and easily producible solution can be achieved. This flexibility in design simplifies the manufacturing process and reduces costs, as it is relatively straightforward to produce pins with varying eccentricity levels. In contrast, aligning other mechanism systems can be more complex and challenging, often requiring more precise and intricate alignment processes.

By utilizing adjustable eccentric pins, it is possible to design fatigue-safe structural components on the aircraft without the need for large holes in primary structures such as the sill longeron. This approach allows for the integration of the locking mechanism without compromising the structural integrity of the aircraft.

The key benefits of this design are multifaceted. Firstly, the use of adjustable eccentric pins eliminates the need for large, potentially weakening cutouts in the sill longeron or other critical structural elements. This not only maintains the structural integrity of the aircraft but also contributes to its overall durability and safety, reducing the risk of fatigue-related failures.

Secondly, this design approach enables the creation of a lighter canopy system. By avoiding large cutouts and minimizing the impact on the sill longeron, the overall weight of the canopy is reduced. This weight reduction has a direct impact on the actuator design, allowing for a lighter and more efficient actuator system.

Furthermore, the simplification of the sill longeron design as a result of this approach contributes to a more streamlined and lighter cockpit design. By reducing the structural complexity and weight of the sill longeron, the cockpit can be designed to be lighter, which enhances the overall performance and efficiency of the aircraft.

In summary, the use of adjustable eccentric pins facilitates a fatigue-safe design by avoiding significant structural modifications. This results in a lighter and more efficient canopy system, a simplified actuator design and a streamlined cockpit, all of which contribute to the overall performance and operational efficiency of the aircraft.

2.2.4 Sideways Canopies

Sideways canopies open by shifting laterally, typically to the left or right side of the cockpit. This design can be advantageous in specific aircraft configurations where side access is preferred or where other opening mechanisms might hinder cockpit ergonomics or visibility. The sideways-opening canopy provides a practical solution for aircraft with unique spatial requirements or design constraints, ensuring that pilot access remains unobstructed and efficient.

CHAPTER 3

METARIALS AND METHOD

The one of usage of pins is to adjust mechanisms structures. Usage of a fixed pin requires additional design efforts and precise tolerance adjustments for whole structure, which impact both the time, cost and effectiveness of the manufacturing and assembly process. Additionally, tolerance deviations may lead to extra preload on the pin during locking which potentially may result a reduced fatigue life for the locking mechanism and low maintainability interval.

Eccentric pin allows to adjustments in sliding mechanisms with different levels of eccentricity. The sliding canopy structure, where rigidity and tight tolerances are essential is the topic of this study.

Instead of using a fixed pin without an alignment or adjustment capability, this study investigates an eccentric pin solution, which allows simple adjustment for critical mechanism. This solution improves the stability of the mechanism by focusing potential impacts, clashes and pretension loads. In this study, the effect of eccentricity in an eccentric pin on the pin's strength was studied.

In this thesis, three different design solutions were investigated for eccentric pins. The first design solution is a single wall (support) eccentric pin. Although its mechanical behavior is similar to the fixed pin, it exhibits worse performance than the fixed pin due to the hole and contact relationship on the housing. In the double-supported eccentric pin structure, the length of the housing was extended to distribute the load more effectively. In the extended double supported eccentric pin structure, the distance between the two support walls was widened by 5 mm.

3.1 Material

Precipitation-hardenable (PH) stainless steels are an important family of steels because they possess a combination of attractive mechanical properties, including high strength, good ductility, fracture toughness and very good corrosion resistance [38].

PH 13-8 Mo, also known as AMS 5629 or by its standard designation 1.4534, is a highly specialized precipitation-hardened (PH) stainless steel. This alloy is distinguished by its exceptional combination of mechanical strength, toughness and superior corrosion resistance, making it a preferred material in critical industries such as aerospace, petrochemical and nuclear engineering. The alloy's unique properties are achieved through a precise heat treatment process that induces the precipitation of fine particles, thereby significantly enhancing its mechanical strength.

The PH 13-8 Mo stainless steel (UNS13800) is a martensitic, precipitation-hardenable stainless steel with corrosion resistance and material characteristics to those of conventional quenched and tempered alloy steels.

Good transverse mechanical properties are a major advantage of PH13-8Mo. PH13-8Mo is produced by double vacuum melting and is available in the form of forgings, plate, bar and wire, normally furnished in the solution-treated (A) condition [39].

A variety of forming, joining and machining processes are usually performed on precipitation hardening stainless steels while the material is in its Condition A stage. This state, which is representative of the material's original state before precipitation hardening, calls for the same tools and production processes as other precipitation hardening stainless steels.

For optimal machinability, it is recommended to use Conditions H1150 and H1150M. Among the several heat-treated states of precipitation-hardening stainless steels, these parameters are recognized to provide the highest machinability properties. Under these conditions the material performs better during machining operations, resulting in manufacturing processes that are more accurate and efficient.

Precipitation hardening of stainless steels results in dimensional changes. For instance, the material experiences a dimensional contraction between 0.0004 to 0.0006 inches per inch after heat-treating to the H1000 state [39].

On the other hand, the dimensional contraction, ranging from 0.0008 to 0.0012 inches per inch, is more noticeable when hardening to the H1100 condition.

These changes in dimensions are important factors to consider during the design and production phases. Their influence can potentially alter the performance and fit of the components in the completed systems by influencing the final dimensions and tolerances of the parts. Therefore, it is crucial to take these contractions into consideration while arranging the production process in order to guarantee that the final goods fulfil the necessary requirements and continue to work as intended.

It is not appropriate to use PH13-8Mo stainless steel in its condition A state; it must only be used in its heat-treated state. Heat treatment is a key factor in determining the material's characteristics and performance since it allows for customization to match different mechanical requirements and strength levels. PH13-8Mo is an alloy with versatility in various applications since it may be heat treated to create a range of characteristics.

Table 3.1 Mechanical properties of PH13-8Mo for different conditions [39]

Specification	**PH13-8Mo (AMS 5629)**	**PH13-8Mo (AMS 5629)**	**PH13-8Mo (AMS 5629)**
Form	Round, hex, square and flat bar	Round, hex, square and flat bar	Round, hex, square and flat bar
Condition	H950	H1000	H1050
Density [kg/m3]	7723	7723	7723
Young Modulus [GPa]	195	195	195
Poisson's Ratio	0.28	0.28	0.28
Tensile Yield Strength [MPa]	1413	1379	1138
Compressive Yield Strength [MPa]	-	1455	-
Tensile Ultimate Strength [MPa]	1524	1434	1207

Table 3.2 Mechanical Properties of PH13-8Mo, PH15-5 and PH17-4 [39]

Specification	**PH13-8Mo (AMS 5629)**	**PH15-5 (AMS 5659)**	**PH17-4 (AMS 5643)**
Form	Round, hex, square and flat bar	Bar and forging	Bar
Condition	H1150	H1150	H1150
Density [kg/m3]	7723	7833	7861
Young Modulus [GPa]	195	197	197
Poisson's Ratio	0.28	0.27	0.27
Tensile Yield Strength (MPa)	931	724	793
Compressive Yield Strength [MPa]	-	683	717
Tensile Ultimate Strength [MPa]	1134	931	924

Engineering stress-strain curves for PH 13-8 Mo stainless steel aged at low, intermediate, and high temperatures (H950, H1050, and H1150) are shown in Figure 3.1. The sample heat-treated to the standard H950 condition demonstrated high strength and relatively low ductility, with rapid necking clearly evident. In contrast, the sample treated under the standard H1050 condition exhibited moderate strength and ductility and showed signs of rapid necking. Meanwhile, the sample heat-treated under the standard H1150 condition displayed lower strength, but significantly higher ductility. Notably, specimens in the H1150 condition also showed considerably higher uniform strains than those in the H950 or H1050 conditions.

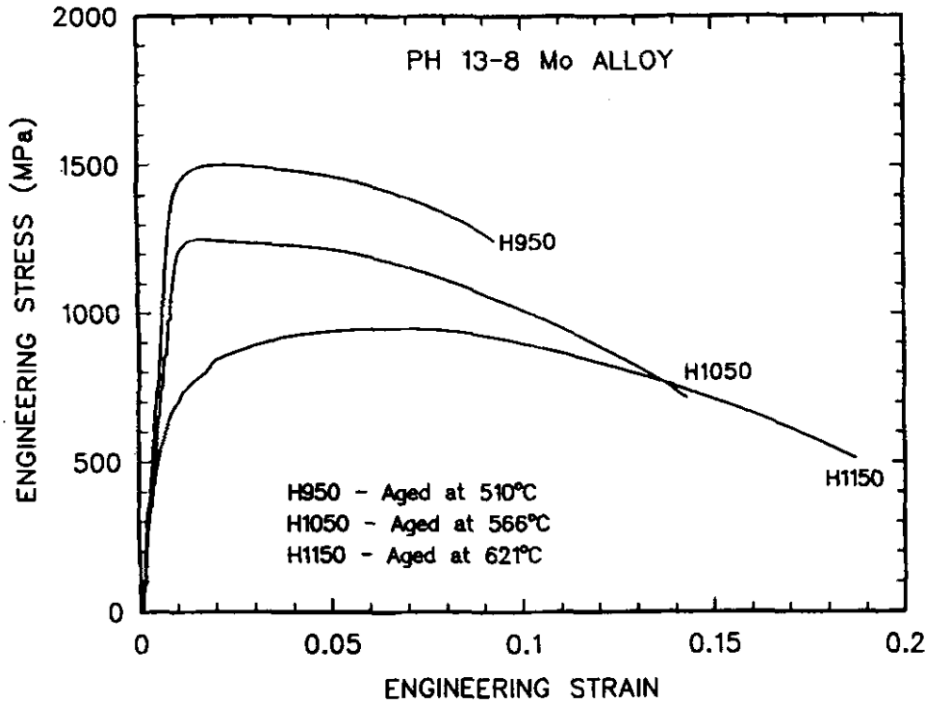

Figure 3.1 Engineering stress-strain curves of cast PH 13-8 Mo stainless steel for different aging conditions [40].

3.2 Methods

Over the past several decades, numerous researchers have conducted extensive investigations on the fundamental causes of friction and wear in materials. Despite the development of numerous theories and models to explain these phenomena, a universally applicable general model for predicting the tribological behaviour of materials in specific situations remains elusive.

The complexity and variability of tribological interactions, influenced by factors such as material properties, surface conditions and operating environments, continue to challenge the formulation of a single, comprehensive model. As a result, while theoretical frameworks and empirical data provide valuable insights, they often require adaptation and refinement to address the unique characteristics of individual applications and scenarios.

For machine components to achieve and sustain optimal performance throughout their

operational lifespan, meticulous optimization of their tribological behaviour is essential. This necessity is particularly critical for components that experience relative motion while interfacing with a countersurface. The interactions occurring at these contact surfaces significantly influence both the reliability and durability of machine components.

Ensuring that components function independently under operational stressors requires the effective management of tribological qualities. It is necessary to ensure precise regulation of wear and friction properties during sliding contact. This process will maximize the components' longevity and efficiency.

If these elements are not managed, they may lead to early failure, reduced efficiency and higher maintenance needs. Therefore, implementing thorough techniques is crucial for optimizing tribological performance. This could involve using precise lubrication procedures, applying cutting-edge surface treatments and choosing the right materials. By successfully handling these factors, machine parts are guaranteed to not only fulfil but also surpass operating requirements, which eventually extends their lifespan and adds to the machinery's overall fidelity and capacity.

Tolerance accumulations are generally addressed with adjustable solutions in systems expected to be both movable and rigid, such as canopies. However, adjustable systems tend to be more complex and heavier, meanwhile eccentric pins offer much more rigid solution in a compact space.

Having a safe and comfortable environment in the cabin for pilots who are well trained and take responsibility for the aircraft as much as the aircraft will increase the safety of the mission and flight. For this reason, environmental control systems balance the cabin pressure at high altitudes and provide a comfortable and safe environment for the pilot and the mission. One of the most critical loads for the canopy is the pressure load applied to the canopy surface at high altitudes. Due to the pressurization, the pressure load affecting the entire canopy surface first reaches the canopy structures and then the canopy locking mechanisms that provide the connection to the cockpit. It is critical for flight safety that the loads on the locking mechanisms must remain below the safe limit and maintain their rigidity during flight. On the other hand, locking

mechanisms that undergo plastic deformation after flight may prevent the canopy from opening or may threaten flight safety in following flights.

Not only is the potential for failure, but also the displacement that occurs with the loads applied during flight are critical for canopy locks. As a matter of fact, the sealing between the canopy and cockpit surfaces is usually provided by an inflatable seal. The maximum inflated height of the seal depends on the type of used seal profile. In case of extreme displacement in the locks, cabin pressure can be lost in a short time.

In this study sliding canopy mechanism divided to different design solutions like fixed design and adjustable design. Adjustable design also divided for single and double support of the housing. A basic view of these combinations can be seen in Figure 3.2.

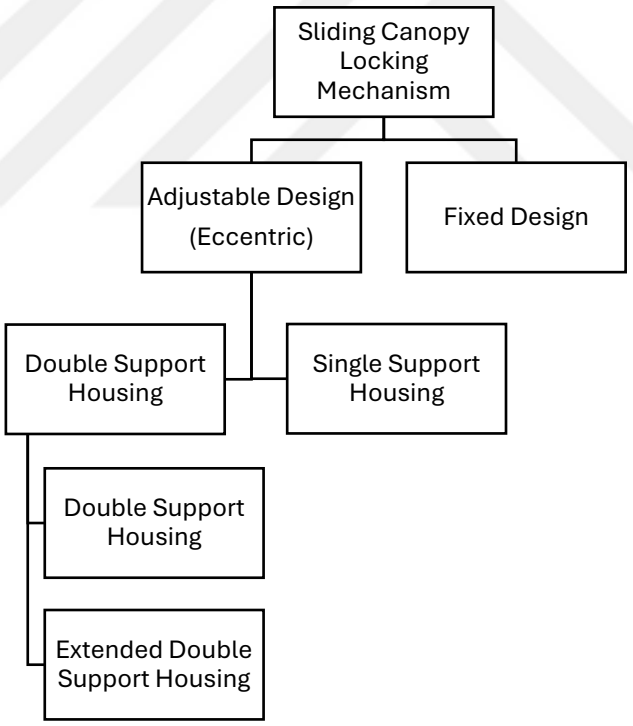

Figure 3.2 Sliding Canopy Locking Mechanism Diagram

The studied locking solutions consist of three main components, excluding the connecting elements. These components consist of an eccentric pin, pin housing and safety self-locking nut.

Table 3.3 Table Eccentric pin dimensions

Parameter	Fixed	Single Wall	Double Wall	Extended Double Wall
L1 [mm]	33	33	33	33
L2 [mm]	-	40	80	80
L3 [mm]	-	2	2	2
D1 [mm]	16	16	16	16
D2 [mm]	-	16	16	16
D3 [mm]	-	30	30	30
E [mm]	-	0-2	0-2	0-2

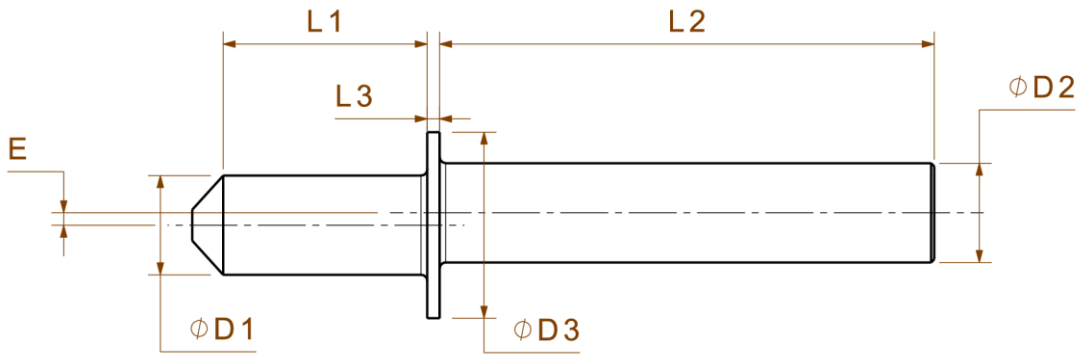

Figure 3.3 Demonstration of an eccentric pin structure with dimensions

Eccentric Pin: It is main element of the locking system. It is designed to provide precise engagement and secure locking through its eccentric design. The eccentric pin is engineered to achieve optimal alignment and stability during operation, allowing for effective locking and unlocking actions with a radius of 5mm. Table 3.3 and Figure 3.3 shows the dimensions of the eccentric pin configurations.

Pin Housing: The pin housing serves as a support structure that houses an eccentric pin. It is designed to hold the pin securely canopy movement and manoeuvring. The housing is constructed to withstand operational stresses and provide a reliable interface between the pin and associated components, which is the canopy frame.

Nut: This is an additional part integrated into the system to complete the locking

mechanism. They are designed to interact with both the eccentric pin and pin housing, ensuring proper alignment and preventing eccentric pin movement. Table 3.4 and Figure 3.4 shows the dimensions of the pin housing configurations.

Table 3.4 Table Pin housing dimensions

Parameter	Fixed	Single Wall	Double Wall	Extended Double Wall
H [mm]	56	56	56	56
W1 [mm]	15	15	15	15
W2 [mm]	-	15	15	15
W3 [mm]	7,5	7,5	7,5	7,5
L [mm]	66,45	66,45	81,2	88,7
G [mm]	-	-	21	26

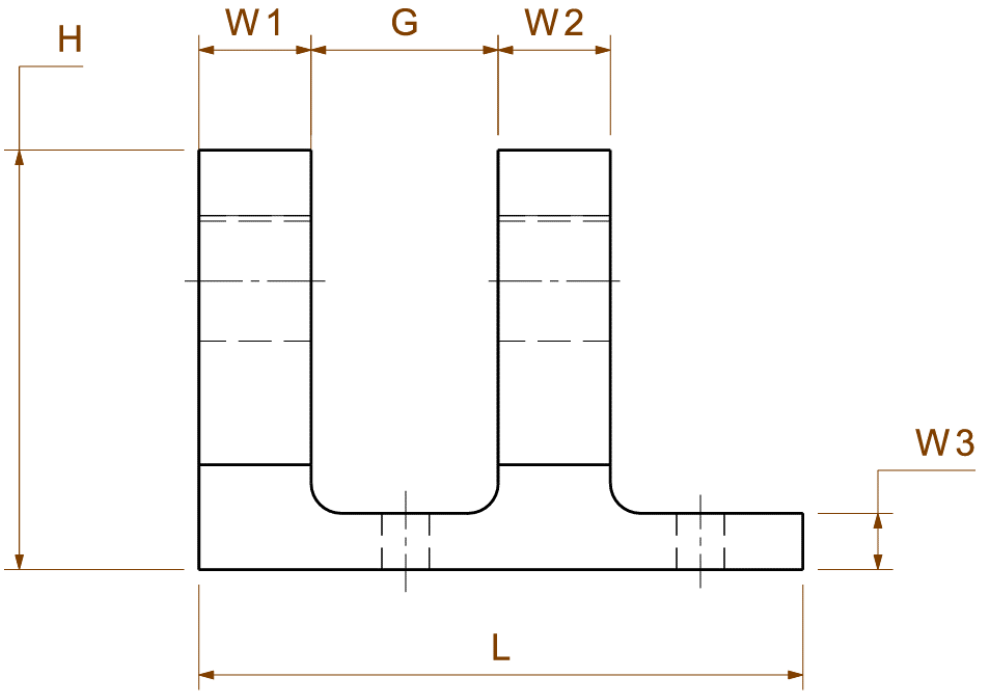

Figure 3.4 Pin housing demonstration with dimensions

The counterpart which is located in the cockpit has not been modelled due to the increased analysis time. Instead, the total surface area of the canopy, combined with

the loads imposed by the aircraft's maximum altitude and the seal pressure, have been calculated.

These loads are then evenly distributed across 10 canopy locking pins. This method simplifies the analysis by distributing the loads equally across 10 canopy pins. It ensures the design can effectively handle the stresses.

Due to the limited gap between cockpit sill longeron and canopy frames, housing parts are limited with ‘H’ heights. Increasing of the H may lead to produce stiffer structures but on the other hand, this may lead to decreasing stiffness of the canopy frames and heavier structures due to locking mechanism moments.

3.3 Finite Element Analysis

Finite element analysis is widely used for displacement and stress analysis. It is very effective in structures where complex interactions takes place. Finite element analysis process consists of creating structure, introducing material properties, meshing structure, applying boundary conditions and loads, solution of problem and processing of results. Tools of these processes is generally given in the type of workflow as shown in Figure 3.5.

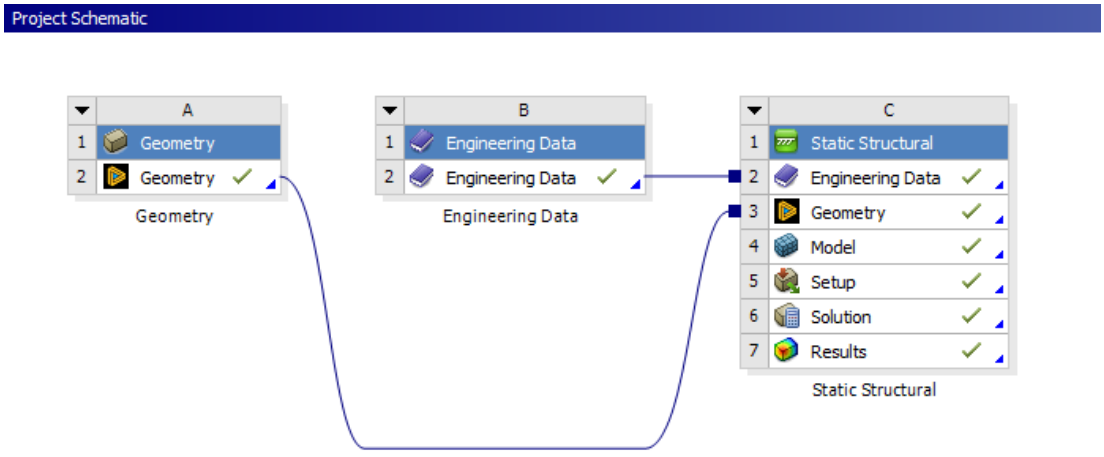

Figure 3.5 Finite element analysis workflow

In this study, ANSYS Workbench program used for finite element analysis. Workflow

of the analysis program can be seen in Figure 3.5.

Chapter A provides a comprehensive overview of the CAD geometry, including both imported and designed elements. This chapter not only details the integration of CAD files but also outlines the modifications that can be made to the CAD data. These modifications are essential for tailoring the geometry to meet specific project requirements and ensuring that the model is accurately represented for subsequent analysis.

In contrast, *Chapter B* focuses on the Engineering Data tool, which is essential for inputting and managing the material properties of the components scheduled for analysis. This chapter details how to utilize the tool to define various material characteristics, such as Young's modulus, Poisson's ratio, density and thermal properties. This ensures that accurate material data are entered, which is crucial for performing precise and reliable component analyses.

The solver applied to the structural problem is the subject of *Chapter C*. The Static Structural solver selected for this study. This chapter describes how this solver combines the geometry from *Chapter A* and the material attributes from *Chapter B* to get the desired output. The combined data from these previous chapters are used by the Static Structural solver to carry out the required computations and generate thorough analytical results.

3.3.1 Creation of Solid Model

In this study, four different locking mechanisms were designed using a commercially available computer-assisted design software, CATIA V5, during the design process.

The created solid geometries were saved and imported in step format for ANSYS finite element analysis software.

The ANSYS Space Claim module is used for additional geometrical improvements and simplifications of solid models.

In this part, creating or importing the geometry of the part or assembly to be analysed. This can involve creating new models or cleaning up and simplifying existing CAD

models to ensure that they are suitable for meshing process.

Simplification: Removing unnecessary details and small features that do not significantly affect the analysis results but can complicate the meshing process is crucial. Otherwise, complex geometrical shapes disturb the mesh geometry and lead to irrelevant results due to poor element quality and increased computational effort. However housing and eccentric pin geometry have been created with significant radius values which may lead to disturb mesh geometry but on the other hand increase the stiffness of the whole structure.

During analysis, all geometries studied for simplification and regular mesh distribution.

In simple terms, a high-quality mesh leads to more accurate results, while a poor-quality mesh can cause convergence issues, potentially resulting in incorrect outcomes and misleading conclusions. Quality of the mesh is changed by factors such as the type of analysis, the time required for meshing and the solving time.

Designed different geometry combinations can be seen in Figure 3.6 and Figure 3.7

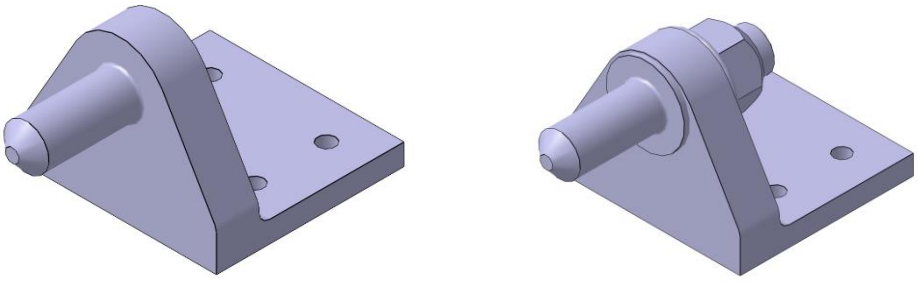

Figure 3.6 (a) Fixed mechanism, (b) single wall supported mechanism

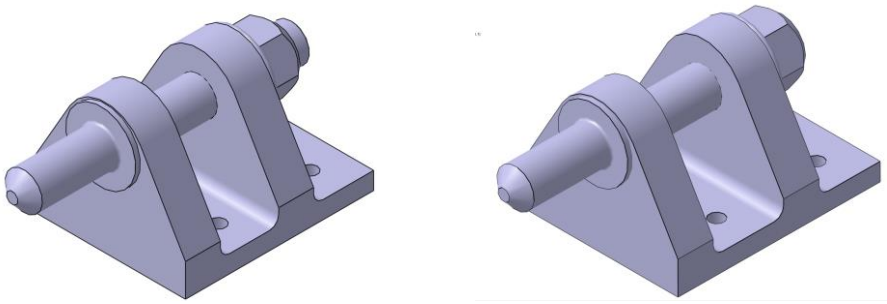

(a) (b)

Figure 3.7 (a) Double wall supported mechanism, (b) Extended double wall mechanism

3.3.2 Material Properties Definition

Material Assignment: Specifying the material properties for the different parts of the model, such as Young's modulus, Poisson's ratio, density and thermal properties, etc. During the analysis process, PH13-8Mo material was assigned as the main structural elements to accurately simulate its mechanical behaviour, including stress and strain responses, under operational conditions. This assignment ensures that the finite element model (FEM) reflects the true performance characteristics of the components, allowing for reliable predictions of the structural integrity, deformation and thermal effects. Material properties defined to ANSYS with creating a new element. Figure 3.8 shows material properties and definition for ANSYS FEA program.

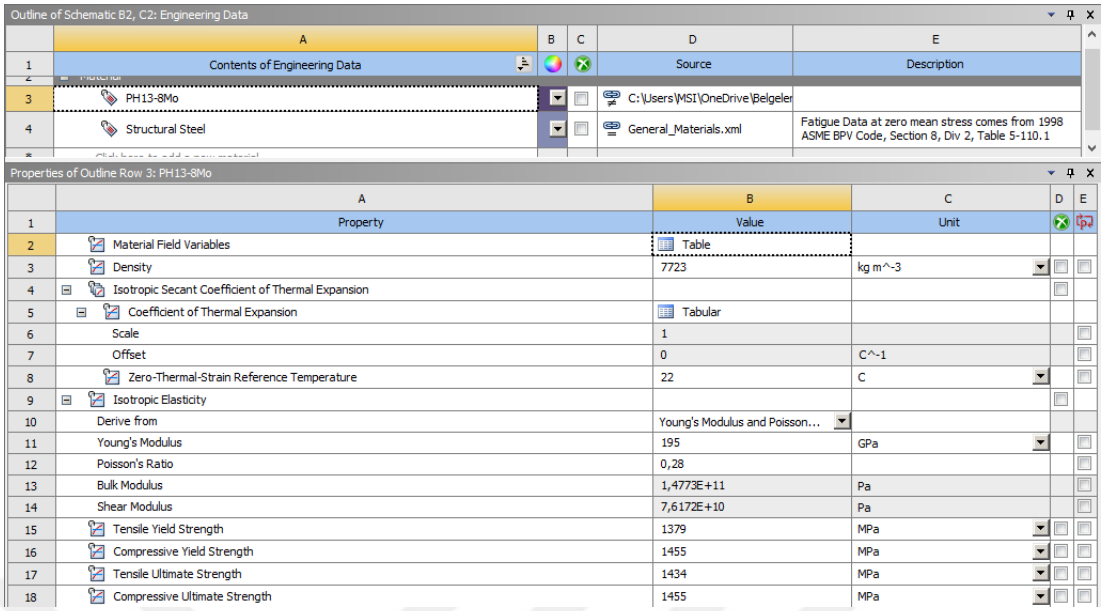

Figure 3.8 Material definition on ANSYS

The necessary coefficients for the PH13-8Mo for the material properties used in the analysis. Table 4.3 shows the mechanical properties of PH13-8Mo material.

Table 3.5 Mechanical properties of PH13-8Mo material [35]

Specification	PH13-8Mo (AMS 5629)
Form	Round, hex, square and flat bar
Condition	H1000
Density [kg/m3]	7723
Young Modulus [GPa]	195
Poisson's Ratio	0.28
Tensile Yield Strength [MPa]	1379
Compressive Yield Strength [MPa]	1455
Tensile Ultimate Strength [MPa]	1434

Nonlinear Material Properties: Defining properties for materials that exhibit nonlinear behaviour, such as plasticity or hyperelasticity, if required by the analysis.

3.3.3 Boundary Conditions

In cruise situation of the aircraft, the external pressure decreases during the climbing phase. Atmospheric pressure, which is against the cabin pressure, causes a pressure difference between the cockpit and the atmosphere.

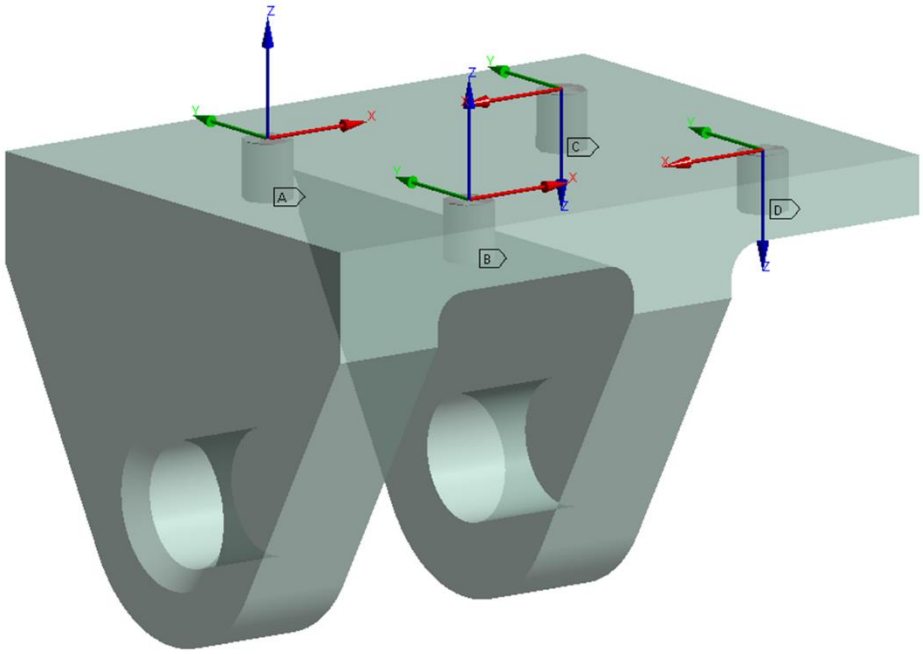

Figure 3.9 Beam elements used for bonding to ground

Thanks to the beam elements, without modelling bolts the main structure effectively bonded to the ground. Without the use of beam elements, the analysis time would have increased and the contact relationships needed to be redefined for each analysis. Figure 3.9 shows the used beam elements and their axis for ground bonding. In this study, bonded surface of the pins located on canopy frame.

3.3.4 Calculation of Effected Loads

The cabin pressure varies according to the cruise altitude of the aircraft. Any altitude over 8000 ft service altitude cabin pressure shall not exceed 18300 ft atmospheric pressure which is equal to 10.92 psi (75262 Pa).

The differential pressure can be calculated using this formula.

$$\Delta P = P_{\text{service altitude}} - P_{\text{atm @18300 ft}}$$

$$\Delta P = P_{\text{atm@55000 ft}} - P_{\text{atm@18300 ft}}$$

$$\Delta P = 1.32 \text{ psi} - 7.24 \text{ psi} = -5.92 \text{ psi}$$

ΔP evaluated as 5.92 psi (41093 Pa)

$$\sigma = \frac{P}{A}$$

To obtain the pressure load, different assumptions must be made in this situation. For this study total Canopy surface area was taken as 2.2 m^2 with 10 locking pins. However, reserve factor (RF) was also taken as 1.5 times of pressure load.

The pressure load shall be calculated as,

$$Applied\ Force = \frac{\Delta P x Canopy\ Surface\ Area x RF}{Total\ number\ of\ Canopy\ Pins}$$

$$Applied\ Force = \frac{\Delta P x 2.2\ m^2 x 1.5}{Total\ number\ of\ Canopy\ Pins}$$

$$Applied\ Force = \frac{41093\ Pa x 2.2\ m^2 x 1.5}{10}$$

$$Applied\ Force = \frac{41093\ Pa x 2.2\ m^2 x 1.5}{10} = 15.410\ kN$$

Each of the canopy pin should carry at least 15.410 kN pressure load during maximum load conditions.

The pressure load was the main load on the pressurized areas. However, owing to the design requirements, the canopy structure can also carry inflatable seal loads.

If the maximum pressure value of the inflatable seal is taken as 1 bar and the perimeter of the canopy structure is taken as 7 m with a seal width of 15 mm, the total seal load can be calculated as;

$$Applied\ Force = \begin{pmatrix} Width\ of \\ the\ seal \end{pmatrix} x \begin{pmatrix} Canopy \\ Perimeter \end{pmatrix} x (Inflatable\ Pressure)$$

$$Applied\ Force = (0.015\ m)x\ (7\ m)x(100000\ Pa)$$

$$Applied\ Force = 10500\ N$$

The force applied by the seal was evaluate as 10500 N.

When applied force divided by canopy pin number to calculate the load for each pin; it will be 1050N will apply to each of the canopy pin.

$$Applied\ Force = \frac{10500\ N}{10pins} = 1050\ N$$

However, the canopy has a weight and maximum negative gravitational force is applied to it to remove it from the fuselage.

If canopy weight taken as 250 kg;

$$Gravitational\ Force = \frac{250\ kg * (3\ g)}{10} = 735{,}8\ N$$

The total force for a single canopy lock is equal to the combination of the pressure, inflatable seal and negative gravitational load.

Total Force = Pressure Load + Inflatable Seal Load + Gravitational Load

13561 N+ 1050 N+735,8 N = 15346.8 N = 15.347 kN.

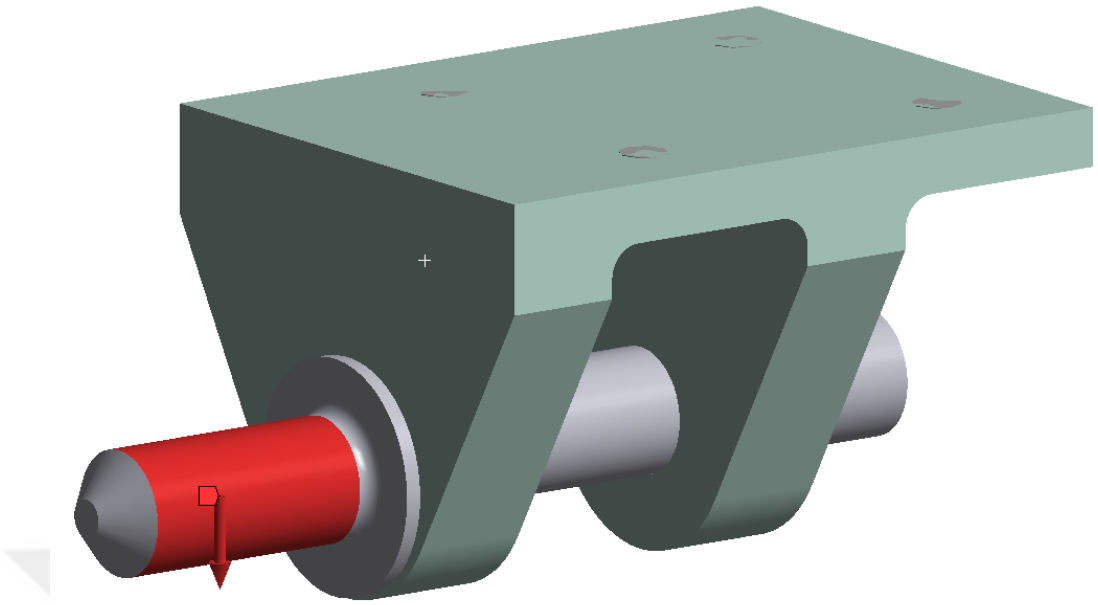

Figure 3.10 Application of the calculated force for each pin

Calculated final force for each pin defined to ANSYS FEA. Force area and its schematic view can be seen in Figure 3.10.

3.3.5 Meshing

Before the analysis, it is necessary to preprocess the designed parts by refining the surfaces. This involves smoothing complex surfaces and simplifying the detailed geometries that does not contribute to the simulation. Such preprocessing ensures that the model is streamlined and free of unnecessary complexity, which helps to improve the accuracy and efficiency of the simulation by focusing only on the relevant features that impact the analysis results.

Mesh Generation: The model is divided into smaller elements that can be solved numerically. This includes choosing the appropriate type and size of elements (e.g., tetrahedral, hexahedral).

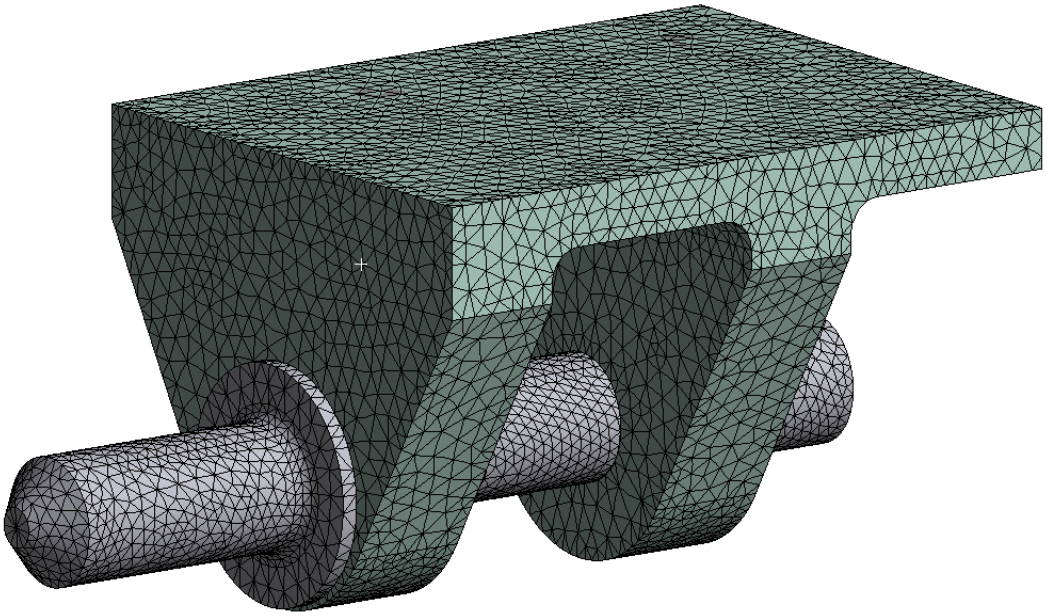

Figure 3.11 Mesh model of double wall supported eccentric pin

Mesh Quality Check: Ensuring that the mesh quality is adequate for the analysis, which may involve checking element shapes, aspect ratios and refinement in critical areas. Figure 3.11 shows the mesh distribution for double wall supported housing and eccentric pin parts.

The von-Mises stress was selected for the mesh independence study. A detailed mesh with an increased number of nodes was utilized for the analysis. The relationship between the number of nodes and the von Mises stress is illustrated in Figure 3.12. For the pin structure, the stress values converge to approximately 1000 MPa with a finer mesh. In contrast, the stress values for the housing structure approach 610 MPa.

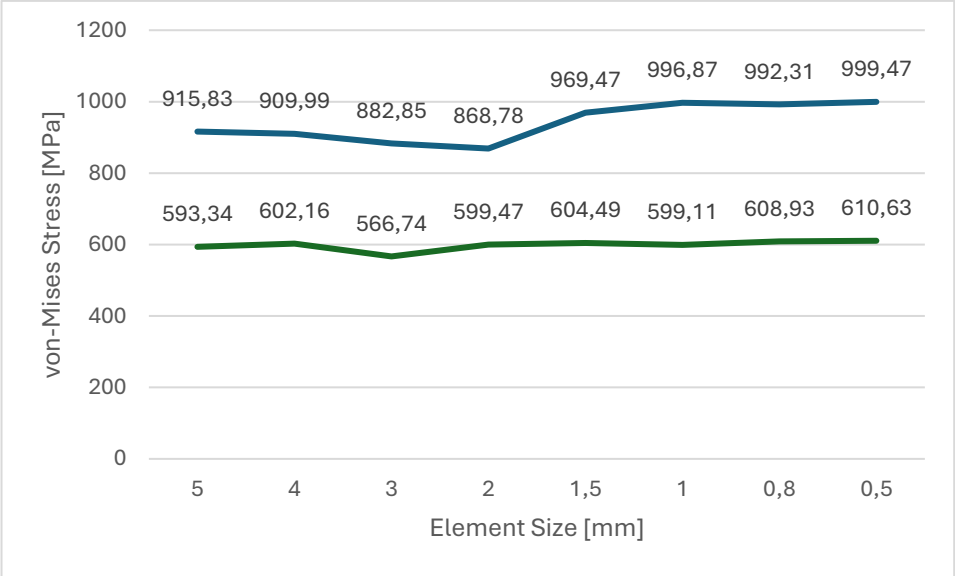

Figure 3.12 Element Size and von-Mises stress relationship

Various element sizes, including 5 mm, 4 mm, 3 mm, 2 mm, 1.5 mm, 1 mm, 0.8 mm and 0,5 mm were considered for the mesh independence study. While smaller element sizes yield a more refined mesh and improved result accuracy, they also substantially increase computational time. Consequently, the optimal element size was determined by analysing stress variations to achieve a balance between computational efficiency and result accuracy.

Therefore 1.5 mm element size has been selected for this study. Stress difference for each element size can be seen in Figure 3.13.

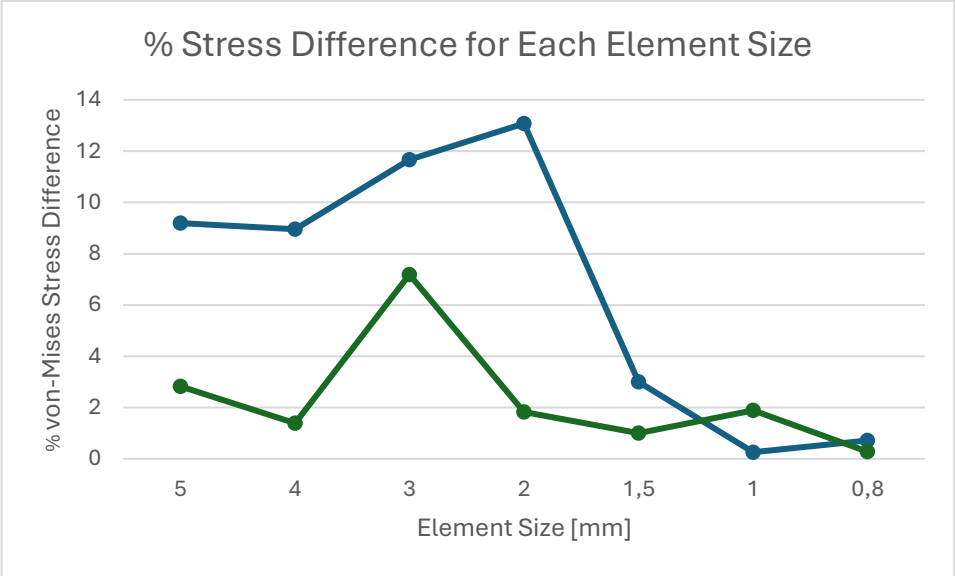

Figure 3.13 Stress difference for each element size

3.3.5.1 Mesh Quality

Mesh quality refers to the effectiveness and accuracy of a finite element mesh in representing the geometry of a model and capturing its behaviour during simulation. In finite element analysis (FEA), the mesh divides the model into smaller, manageable elements (such as triangles, quadrilaterals, tetrahedra or hexahedra), which are used to approximate the physical properties and responses of the structure. High mesh quality is crucial for obtaining accurate and reliable simulation results.

Key aspects of mesh quality shall include Element Shape and Size, Element Density and Smoothness. In this study, the element size was restricted to 1,5 mm for each analysis to ensure accurate results.

3.3.5.1.1 Stress Singularity

Stress singularities often shown in simplified geometric models when certain conditions lead to unrealistic scenarios. These singularities occur because in regions where the area approaches zero, the stress theoretically becomes infinite. This phenomenon happens due to stress is defined as force divided by area (P = F/A). When a CAD geometry introduces discontinuities or sharp features, it can lead to stress singularities in finite element analysis (FEA). These singularities result in extremely

high stress values that are not physically realistic, typically due to the simplification of the model and the corresponding reduction in the area over which the load is distributed. One of this stress singularity for housing element can be seen in Figure 3.12.

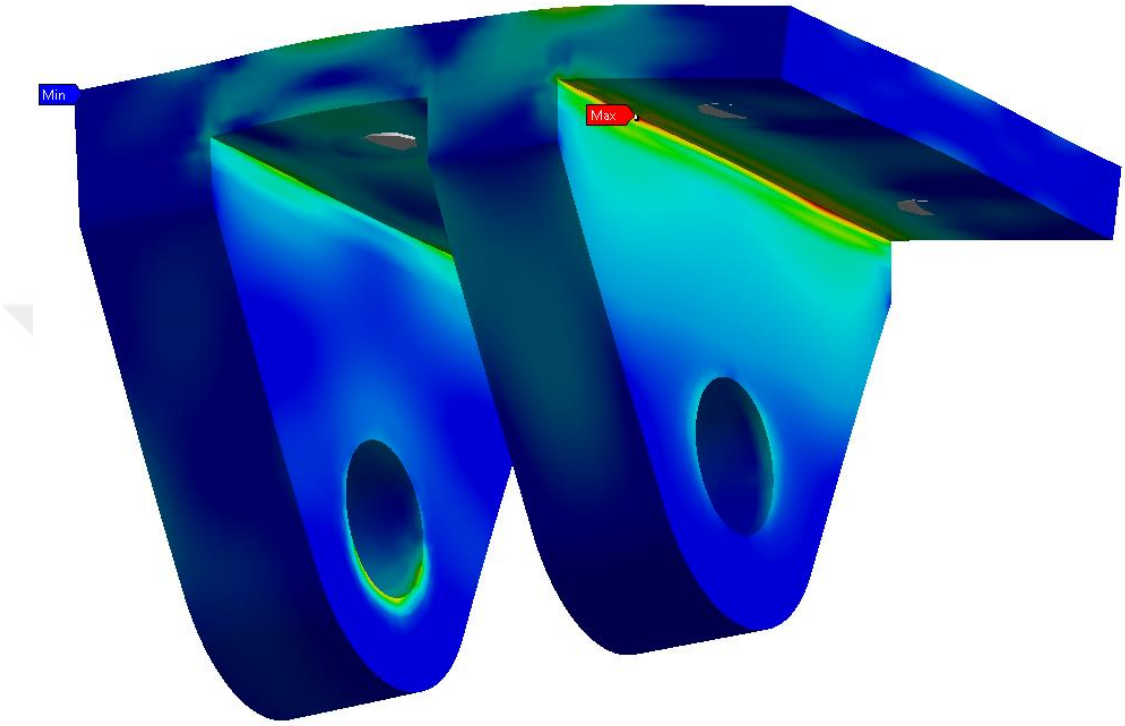

Figure 3.14 Stress distribution of point and pressure load

3.3.5.1.2 Stress Concentration

The global vertical stress contour over the nominal applied stress at the top is shown in the image below. An equation for planar stress has been used to model the L structure. It is evident that the corner experiences the highest tension and compressive loads. As a result, as the mesh is refined, the maximum and minimum stresses of the body will always increase with mesh refinement.

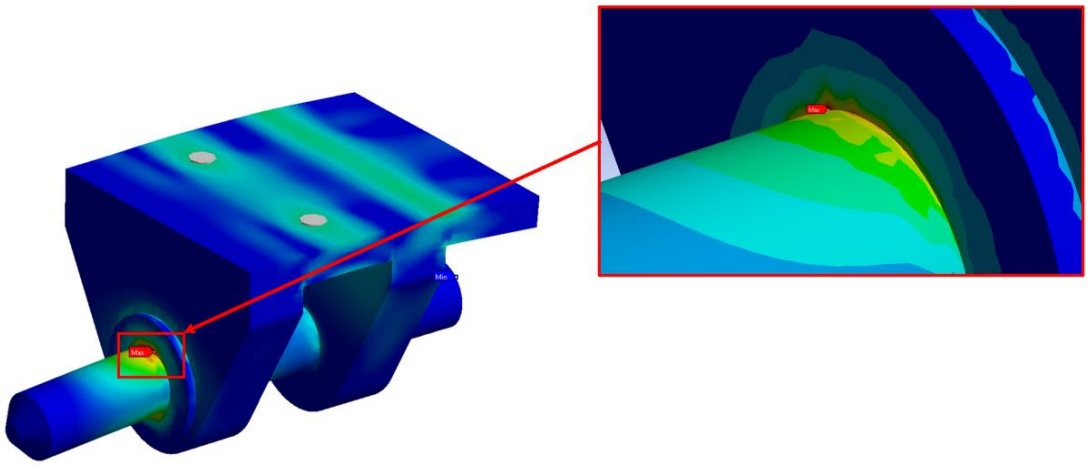

Figure 3.15 Typical sharp corner of 90º – Contour of the stress singularity and its local effect.

In reality, no corners can be precisely sharp. Machining always leaves a little fillet radius on a manufactured sharp corner, even if that is what is required. This indicates that the corner singularity disappears and the tension will no longer be infinite. An example can be seen in Figure 3.13 of this stress concentration.

After discussions, these corners have been updated with 2 mm radius value to get realistic results. The increase in the fillet value has resulted in stress values that are significantly more stable and meaningful, and that supported to enhancing the reliability of the analysis.

3.3.5.1.3 Element Quality and Skewness

To improve the quality of the mesh, it is essential to avoid low orthogonal quality and high skewness values. In the present study, the distribution of element quality and skewness values were analysed.

Skewness mesh metrics spectrum

Excellent	Very good	Good	Acceptable	Bad	Unacceptable
0-0.25	0.25-0.50	0.50-0.80	0.80-0.94	0.95-0.97	0.98-1.00

Figure 3.16 Skewness mesh spectrum

If the skewness mesh metric exceeds 0.95, the mesh is considered to be of poor quality and unacceptable, which could lead to unrealistic results. In addition, element quality was carefully considered during this study. The target value for element quality was set at 1.0 value and the overall average element quality was asserted at greater than 0.75 value to ensure reliable and accurate results.

3.3.6 Pre-Processing Effects

Accuracy of Results: In finite element analysis (FEA), precise geometry development, accurate material definitions and high-quality mesh generation are necessary to achieve accurate results.

Computational Efficiency: By minimizing the amount of time and resources needed for analysis while retaining the accuracy of the results, simplifying the geometry and fine-tuning the mesh can significantly improve computational efficiency.

Model Stability: For realistic simulation results, it is imperative to ensure model stability. This is accomplished by precisely describing the loads and boundary conditions, which aids in the expected behaviour of the model under simulated circumstances. Boundary conditions and loads that are appropriately set are essential to avoid numerical instabilities and preserve the model's stability and dependability during the analysis process.

Analysis of the Results: The quality of the model's preparation and pre-processing has a major impact on how accurately and clearly the results are interpreted. The interpretation of analysis results can be made more efficient and trustworthy with a well-prepared model that includes well defined geometry, material properties and mesh features. This thorough technique guarantees that the outcomes are in line with the anticipated physical behaviour of the model, simplifying the validation procedure and improving the overall.

In conclusion, the pre-processing stages in FEA are important for providing the precision, effectiveness and dependability of the analysis.

In this study, certain simplifications were applied to the solid model geometry to

achieve a more uniform mesh distribution.

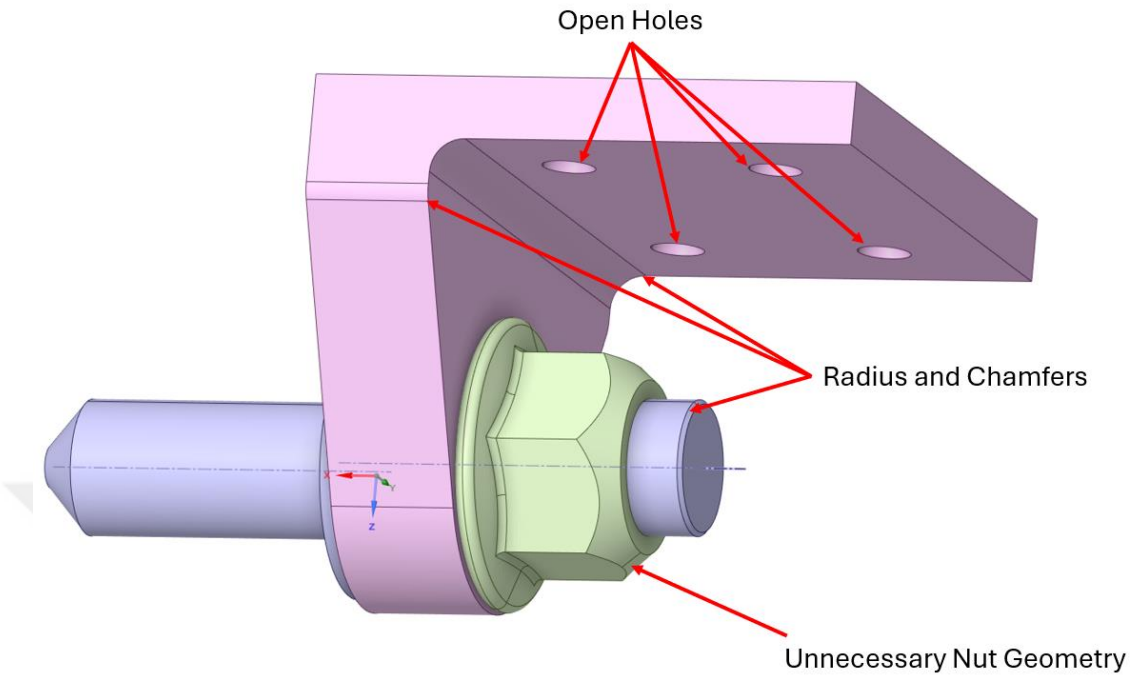

Figure 3.17 Complex state of the solid model

The initial complex state of the solid model can be seen in the Figure 3.14.

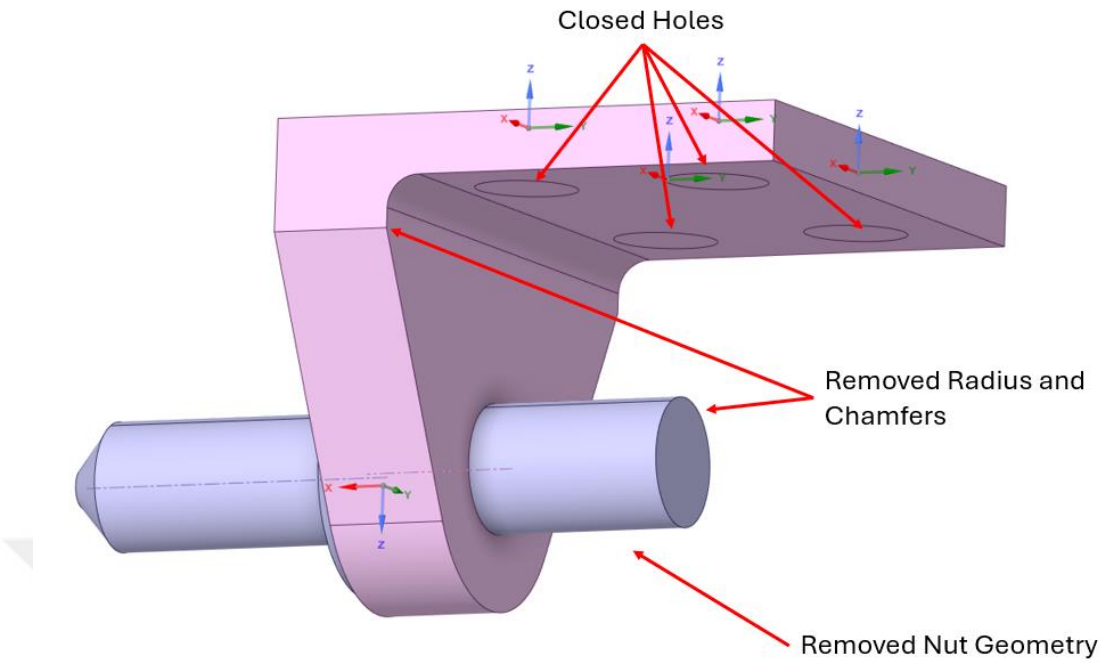

Figure 3.18 Simplified state of the solid model

The final, simplified and refined geometry for the analysis is shown in the Figure 3.15.

These simplifications were made to enhance the efficiency and accuracy of the mesh generation process, ensuring that the mesh was adequately refined while maintaining the computational feasibility. By streamlining the geometry, a more consistent and manageable mesh can be produced, which facilitates better analysis and results.

3.3.7 Contact Type

Defining a contact relationship between two interacting models is crucial during finite element analysis.

Assigning a contact relationship between the eccentric pin and housing model is important because they are independent of each other. The bonded contact type can be assigned for the model interaction if it is assumed that the two models cannot be separated from each other and cannot be seen any sliding motion. With this type of contact, the analysis is made simpler while still precisely reflecting the desired interaction between the pin and housing, which is guaranteed to be in a rigid

relationship with no relative movement. Moreover, to catch realistic result no-seperation and frictionless contact types have been defined for related surfaces. Thanks to no-seperation contact type, there is no gap between indicated surfaces but sliding motion has allowed. The cylindrical shape of the pin cannot separate out but can slide without resistance on the support of the housing part.

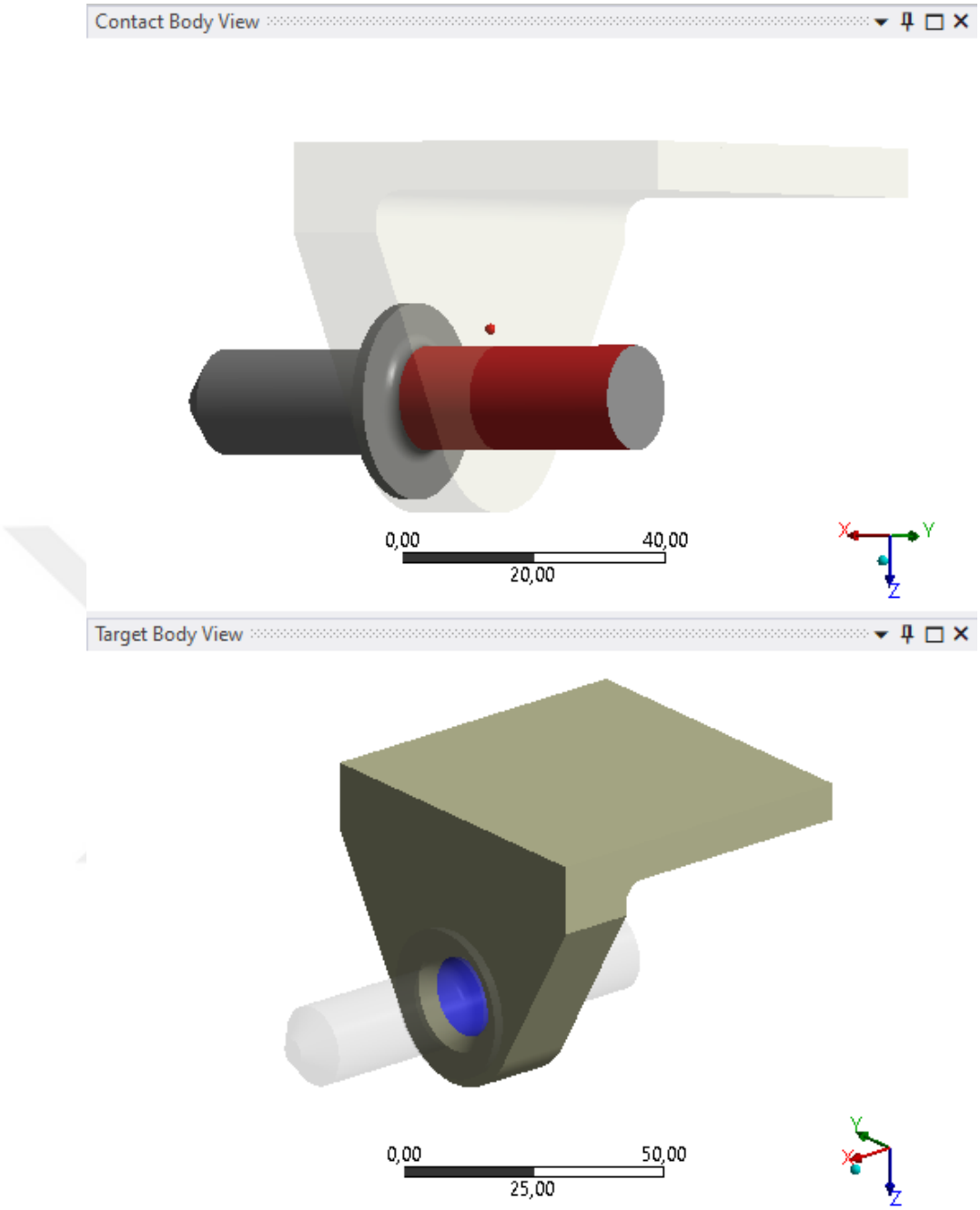

Figure 3.19 Master and slave bodies for no separation contact relationship

The master-slave contact type is a technique used in finite element analysis to control the interactions between two touching surfaces, where one surface is identified as the "master" and the other as the "slave." The slave surface adjusts to the restrictions of the master surface, whereas the master surface, which is usually stiffer or finely meshed, regulates the contact interaction. When there is a noticeable variation in the

stiffness or mesh quality between the surfaces, this method works especially well. This sort of contact improves accuracy and computational efficiency by confirming that the slave surface matches the master surface and prevents penetration. It is essential for realistic simulations and makes contact calculations easier, particularly in situations where one surface is significantly stiffer or has a finer mesh than the other. Defined master and surfaces can be seen in Figure 3.19 and Figure 3.20.

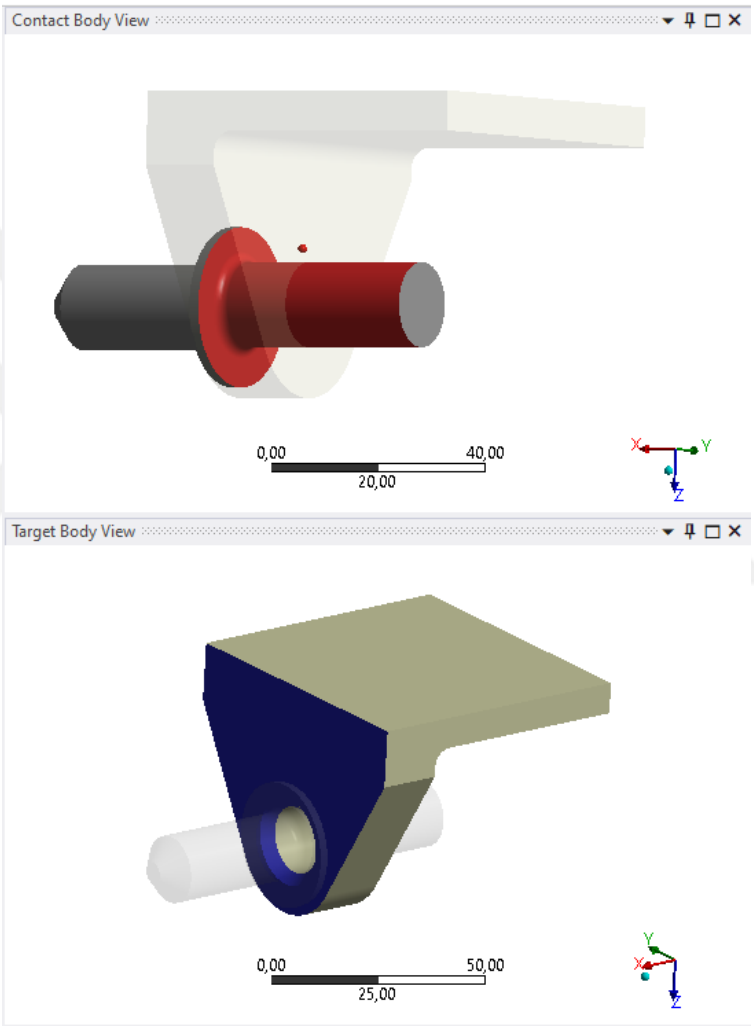

Figure 3.20 Master and slave bodies for frictionless contact relationship

The eccentric housing is structurally stiffer than the pin and has been given a more detailed mesh in this study. For the purpose of defining the contact, the pin was identified as the slave geometry, while the housing itself was chosen as the master (target) geometry.

CHAPTER 4

RESULTS AND DISCUSSION

4.1 Deflection Values

Based on the analyses, the single wall eccentric pin experiences the highest deflection value among the various pin types evaluated. When ranking these pins from the greatest to the least deflection, the sequence is as follows: the single wall eccentric pin shows the most significant deflection and followed by the fixed pin, which has a lower deflection value but is still considerable. The double wall eccentric pin, which shows less deflection than the extended double wall eccentric pin and the single wall eccentric pin. Average deflection results and pin type relationship can be seen in Table 4.1.

Table 4.1 Average Deflection Values Based on Design

Parameter	Fixed	Single Wall	Double Wall	Extended Double Wall
Average Deflection (mm)	2,506	2,859	1,725	2,021

The pin with the minimum deflection was the double wall eccentric pin, which demonstrated the smallest amount of displacement under same load. This ranking highlights the varying degrees of deflection endured by each pin type under identical loading conditions. The gradient of the deflection values for the investigated solution is shown in Figure 4.1-4.4.

The average deflection values were significantly abnormal for the fixed or single wall solutions. The average deflections of the fixed pin and single wall solutions were calculated as 2,570 mm and 2,859 mm respectively. Due to the inflatable seal and tolerance stacking, the minimum deflection values are preferred for latching mechanisms. Figure 4.1 and Figure 4.2 show the nominal and deflected structures with local minimum and maximum locations.

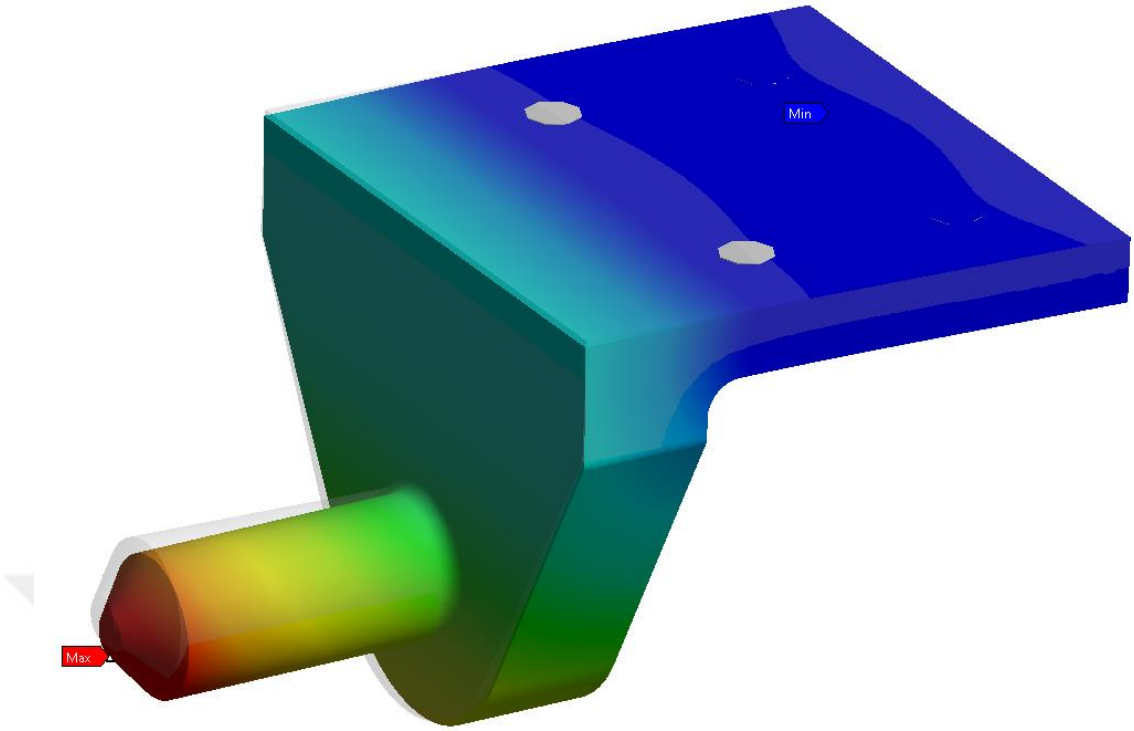

Figure 4.1 Total deflection gradient for fixed pin solution

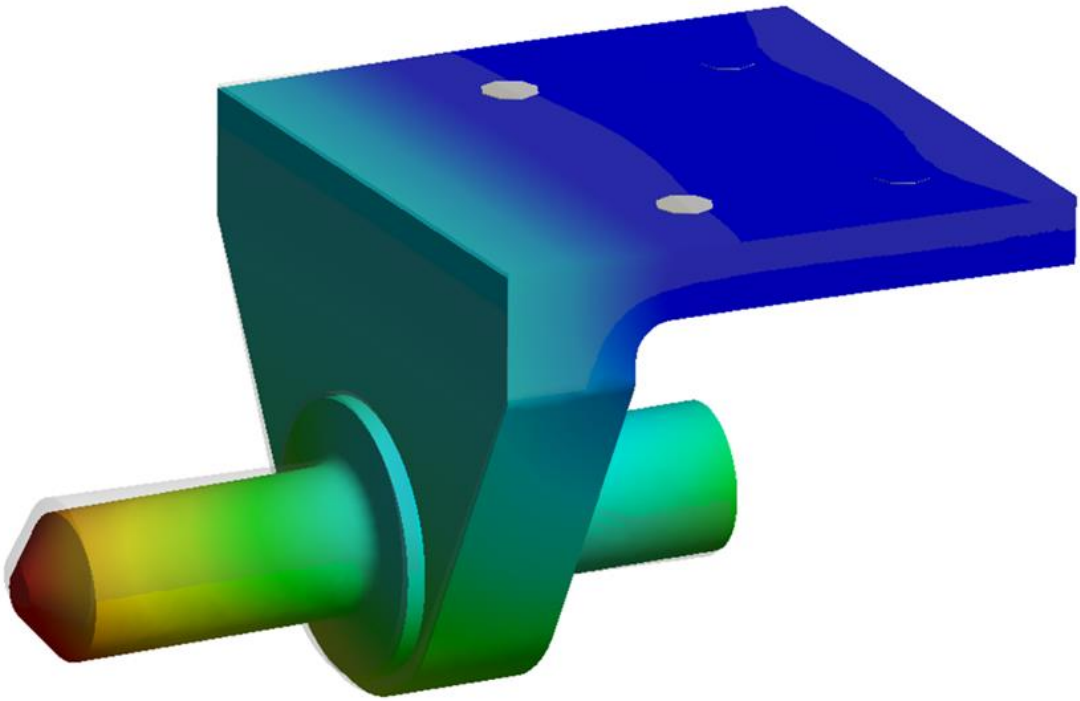

Figure 4.2 Total deflection gradient for single wall eccentric pin

However, the average deflections of double wall and extended double wall solutions, calculated as 1,725 mm and 2,021 mm which are significantly lower than those of the previous designs. Deflection gradients for double wall and extended double wall solutions can be seen in Figure 4.3 and Figure 4.4 respectively.

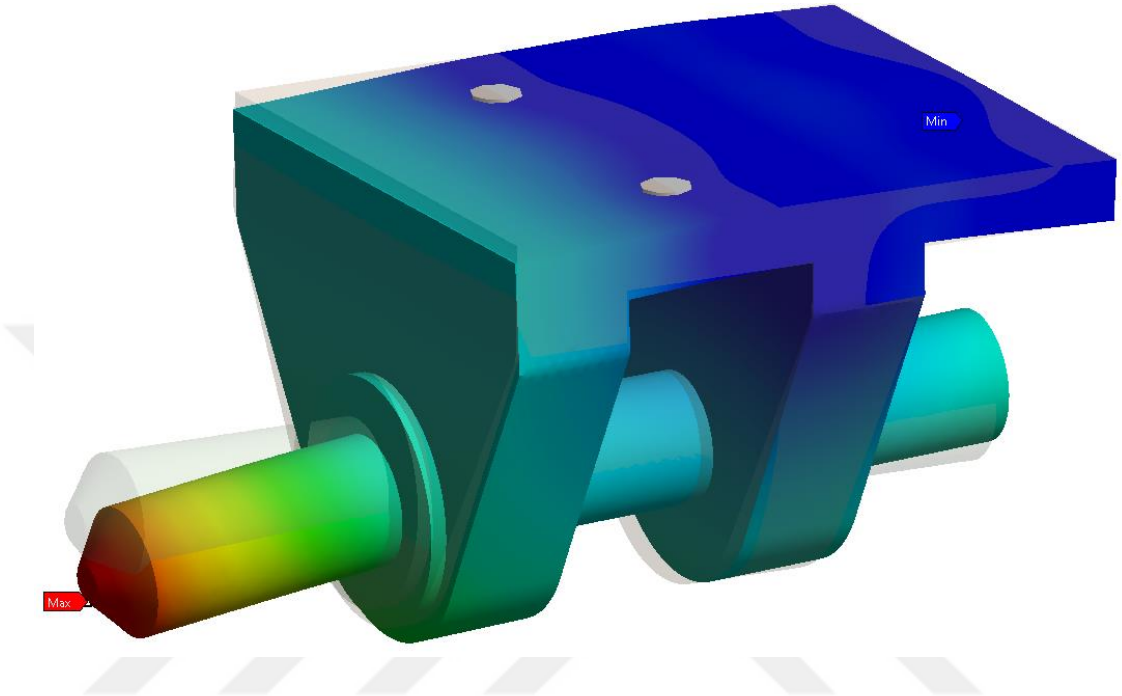

Figure 4.3 Total deflection gradient for double wall eccentric pin

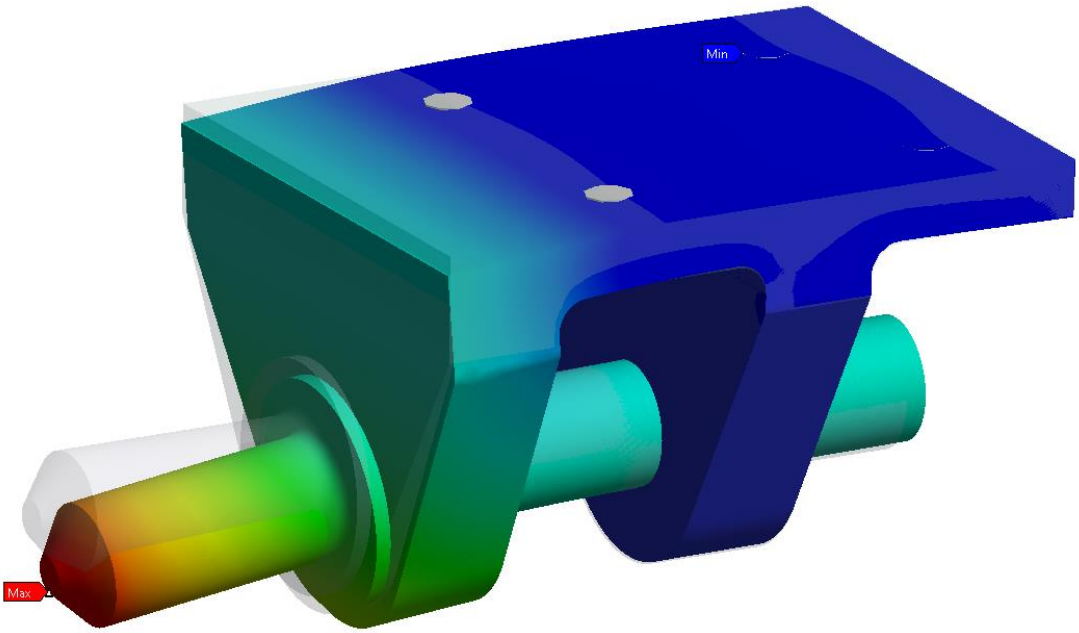

Figure 4.4 Total deflection gradient for extended double wall eccentric pin

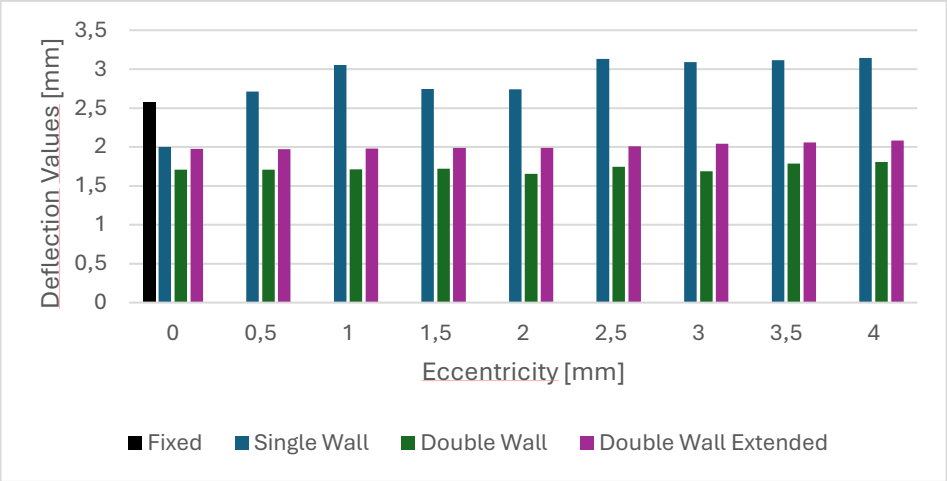

Figure 4.5 Results of total deflection based on eccentricity levels

The double wall and extended double wall models can be used in designs where deformation values are critical. It is crucial to understand how deflections affect the overall body and functionality of the mechanical system. In case to stress values, critical deflection occurs on pin body and effects the overall solution. Therefore, only pin deflection values investigated and compressed in this study. Deflection results and eccentricity relationship for each solution are presented in Figure 4.5. According to Figure 4.5 increasing eccentricity of the pin structure are not affect to deflection value. This may a result of low eccentricity values that does not affect the mechanical behaviour of the pin structure.

4.2 von-Mises Stresses

Doble wall and extended double wall solutions have the minimum von-Mises stress value almost each eccentricity level. Table 4.2 presents a comparison of average von-Mises Stress results and pin type relationship. All of the calculated stress values were lower than the yield strength of the material. However, the pin body is subjected to higher stress levels compared to the housing body due to its critical role in transmission of the bending load and load bearing within the assembly.

Table 4.2 Average von-Mises stress values based on design

Parameter	**Fixed**	**Single Wall**	**Double Wall**	**Extended Double Wall**
von-Mises Stress for Pin (MPa)	1183,8	1259,83	1228,14	1244,38
von-Mises Stress for Housing (MPa)	-	1098,70	605,48	666,68

The double wall and extended double wall eccentric pin solutions have the minimum stress value, which also demonstrated the smallest amount of displacement under same load. To rank the solutions from minimum to maximum, there is no clear ranking; however, the double wall eccentric pin and extended double wall eccentric pin solutions have a significantly lower stress level than single wall supported pin for different eccentricity values.

Based on the analysis, it was observed that the location of the maximum von-Mises stress was the boundary of the front fasteners for the fixed and single-wall eccentric pin solutions. An additional wall effectively reduced the stress values on the housing part in the case of the fixed and single wall eccentric pin solutions. Figure 4.6 and Figure 4.7 includes an illustration of von-Mises stress distribution for fixed and single wall solutions.

Thanks to the additional wall support, the maximum stress value can be seen on the eccentric pin for the double supported solutions. The maximum stress locations can be seen in Figure 4.8 and Figure 4.9 for double wall and extended double wall solutions.

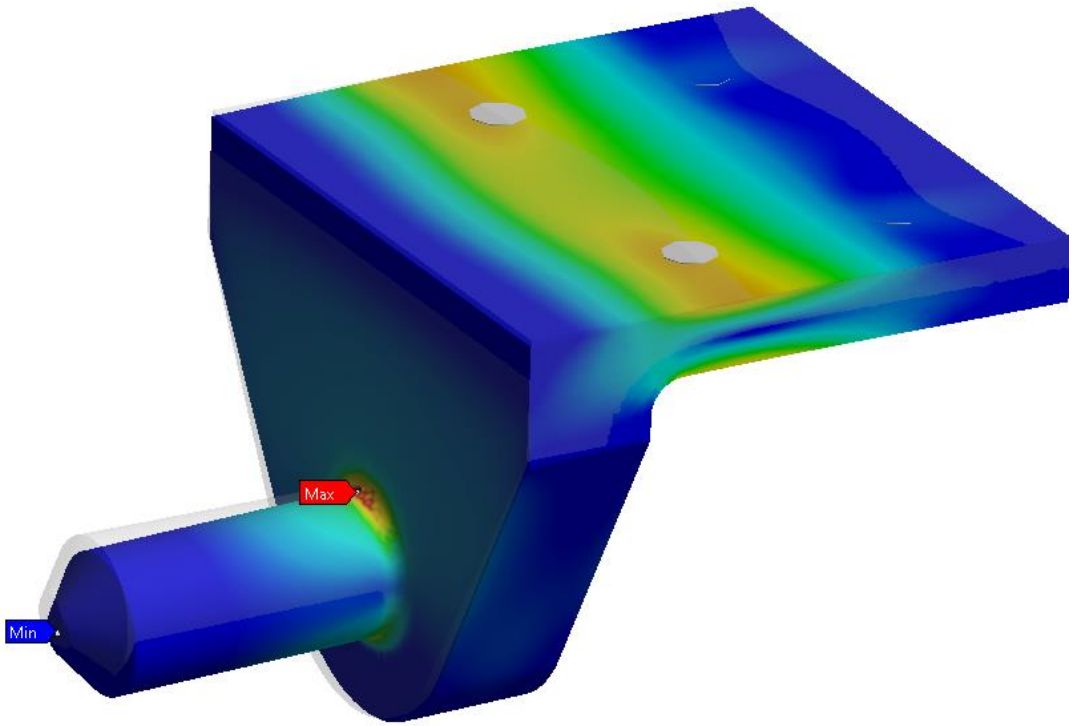

Figure 4.6 von-Mises stress distribution on fixed pin solution

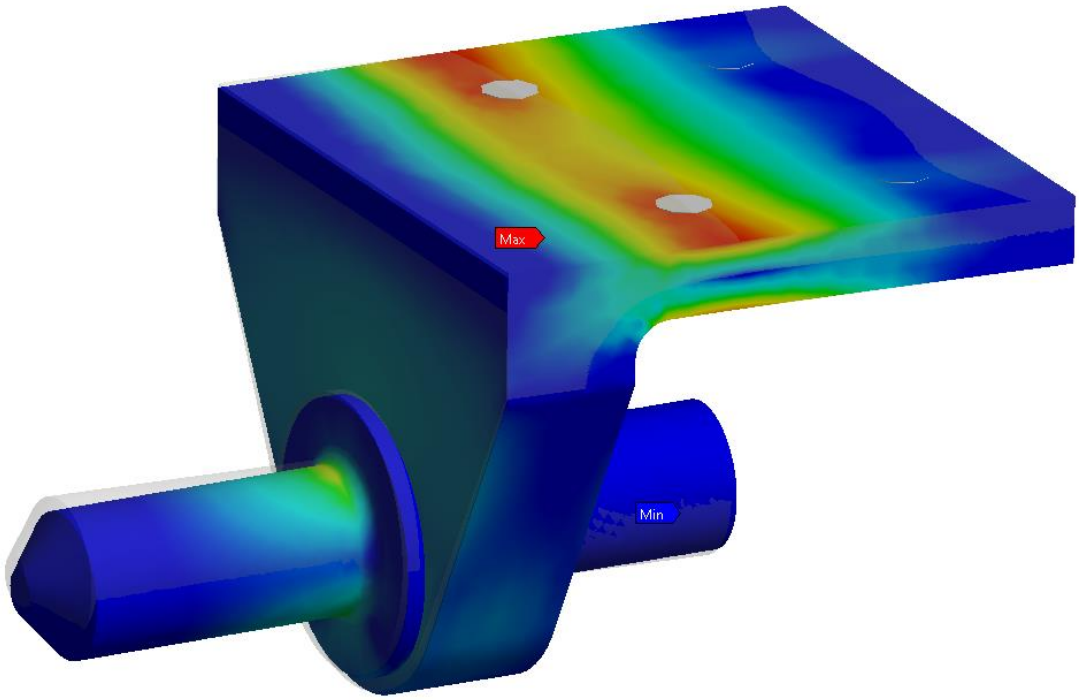

Figure 4.7 von-Mises stress distribution on single wall eccentric pin

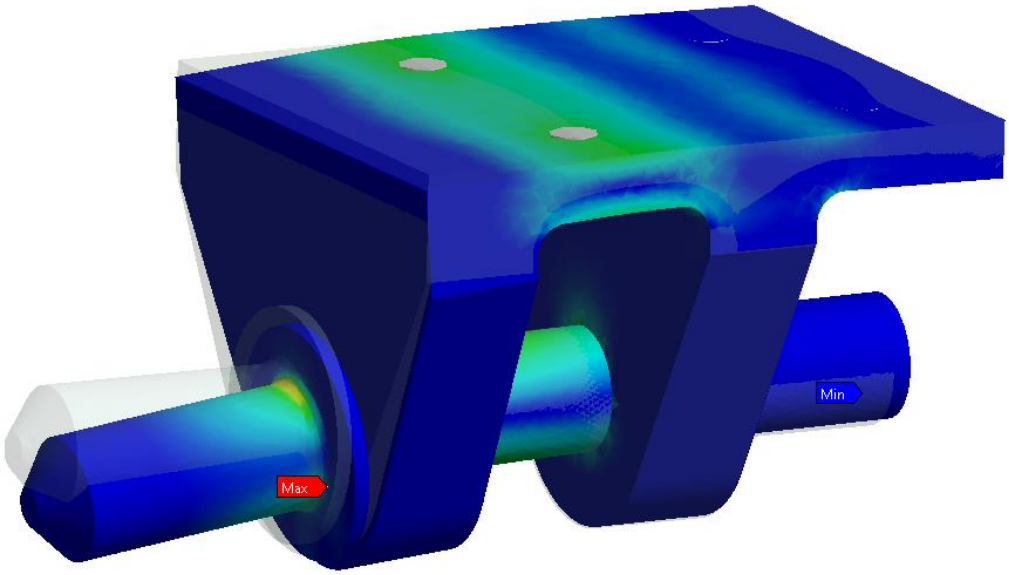

Figure 4.8 von-Mises stress distribution on double wall eccentric pin

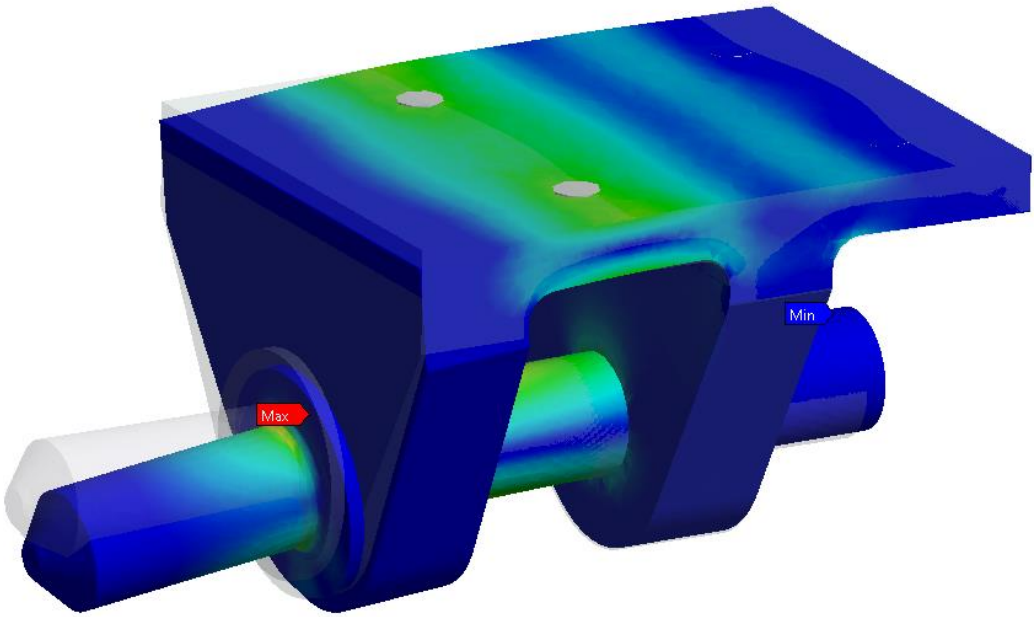

Figure 4.9 von-Mises stress distribution on extended double wall eccentric pin

Moreover, the magnitude of the eccentricity did not affect the von-Mises stress values for pin structure for lower eccentricity levels like 0-2 mm. However, increased eccentricity may affect structural stability which can be shown in Figure 4.10.

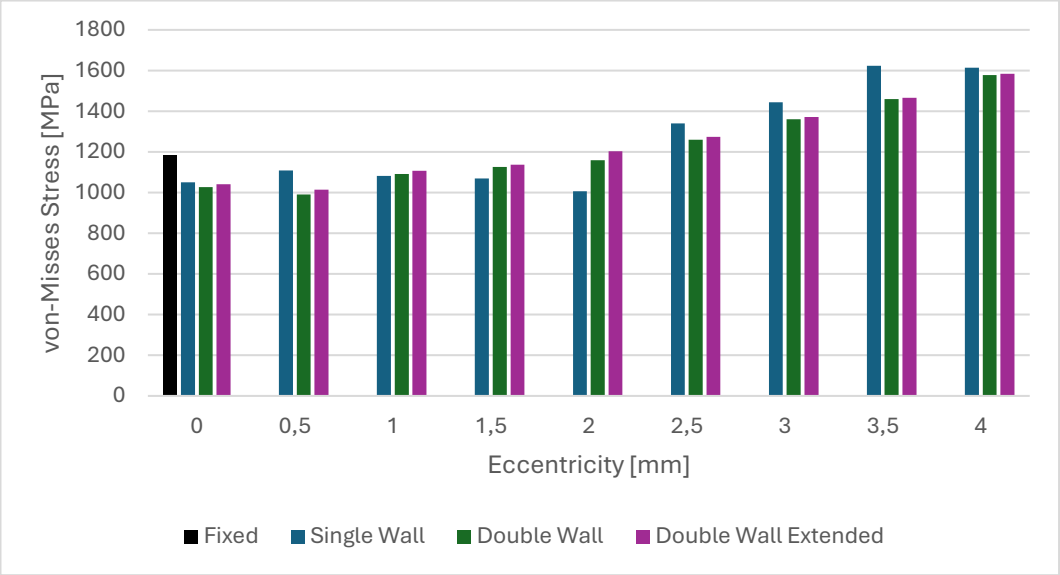

Figure 4.10 von-Mises stress distribution based on eccentricity levels for pin structure

Despite no noticeable differences were observed in the pin structure, it was found that as the eccentricity increased, von-Mises stress values began to decrease for double supported bodies in the housing structure as shown in the Figure 4.11.

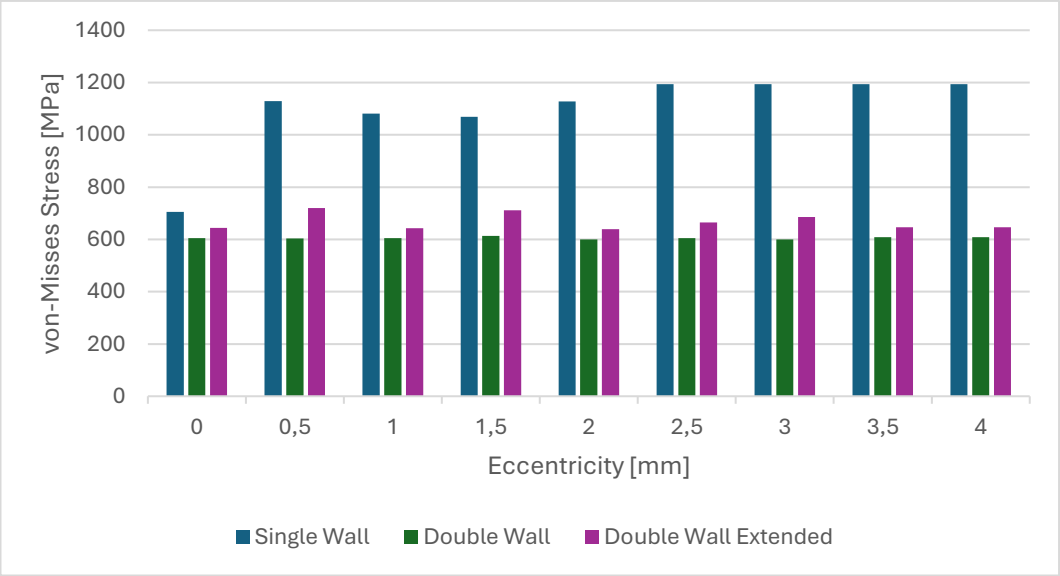

Figure 4.11 von-Mises stress distribution based on eccentricity levels for housing structure

The different levels of eccentricity can significantly impact the stress distribution in both the pin and the housing surfaces. For instance, Figure 4.12 illustrates the stress distribution in double wall extended housing structures with 0 mm and 2 mm eccentricity. In the Figure 4.12b, front wall stress distribution is more spread unlike the Figure 4.12a uniform stress distribution.

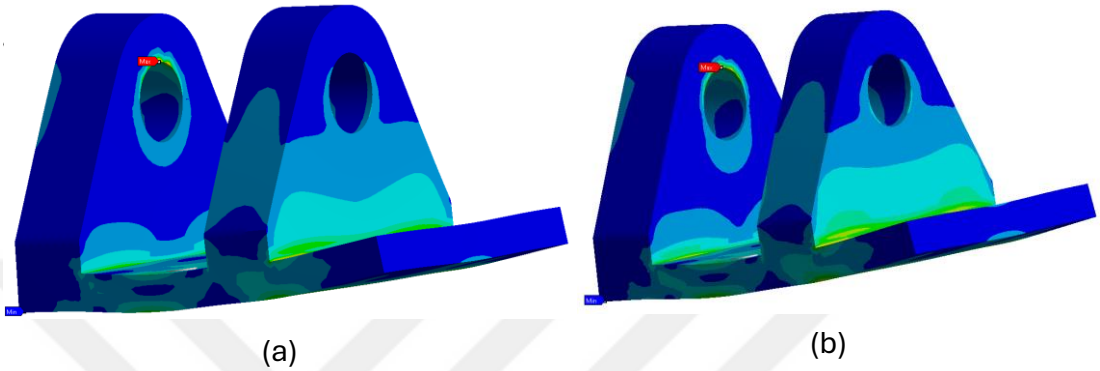

Figure 4.12 von-Mises stress distribution for (a) linear pin structure and (b) maximum eccentric pin, double wall extended housing structures

4.3 Maximum Principal Stresses

The Maximum Principal Stress values were lower for the fixed geometry, whereas the single and double wall design exhibited the highest average values.

Table 4.3 Maximum principal stress values based on design

Parameter	Fixed	Single Wall	Double Wall	Extended Double Wall
Maximum Principal Stress for Pin [MPa]	1339,2	1462,44	1403,97	1407,38
Maximum Principal Stress for Housing [MPa]	-	1206,43	695,54	712,49

As summarized in Table 4.3, the single wall eccentric pin housing structure has significantly high stress values compared to double supported structures.

The fixed wall design shows the highest principal stress values and followed by the

single supported pin configuration. However, both designs have stress concentration issues around the first-row fasteners, as shown in Figure 4.13 and Figure 4.14, where the minimum and maximum stress values represented on the part.

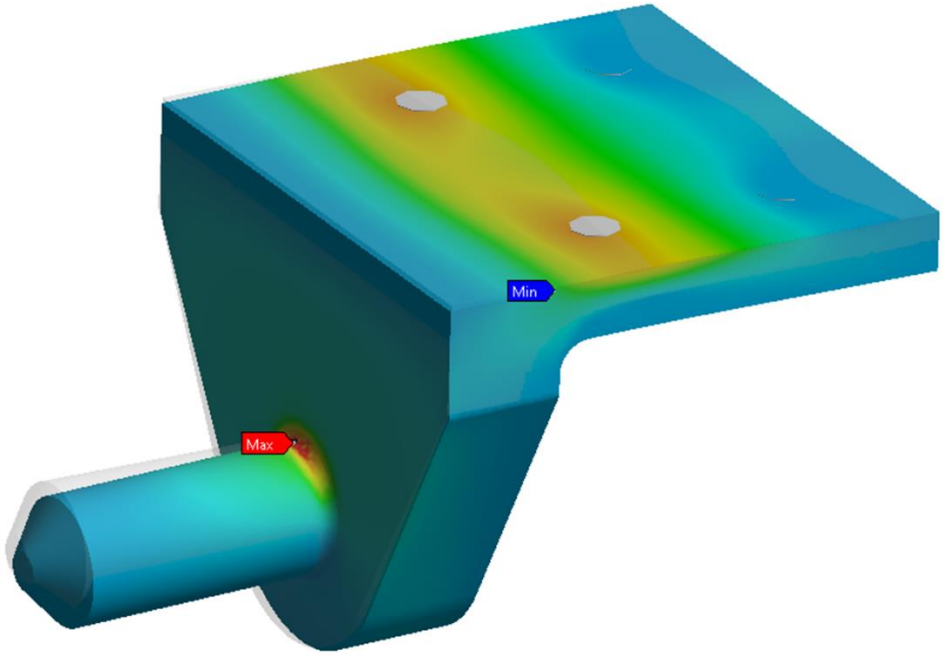

Figure 4.13 Maximum principal stress distribution on fixed pin solution

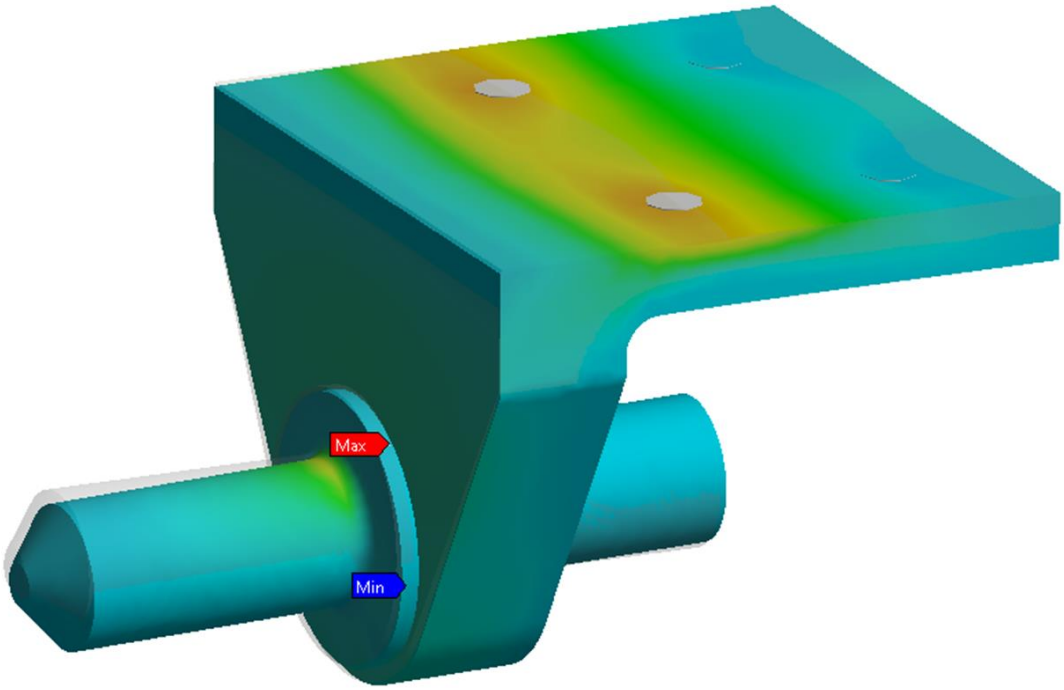

Figure 4.14 Maximum principal stress distribution on single wall eccentric pin

As expected, maximum stress location moved from first-row fasteners to pin surface for double wall design solutions. Both of the stress gradients of the double wall design solutions are shown in Figure 4.15 and Figure 4.16.

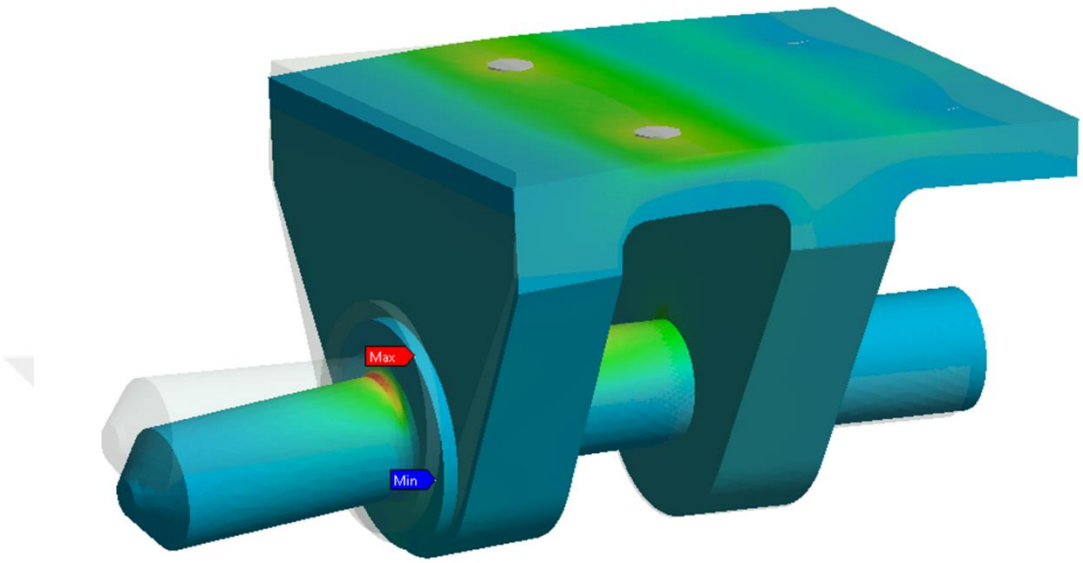

Figure 4.15 Maximum principal stress distribution on double wall eccentric pin

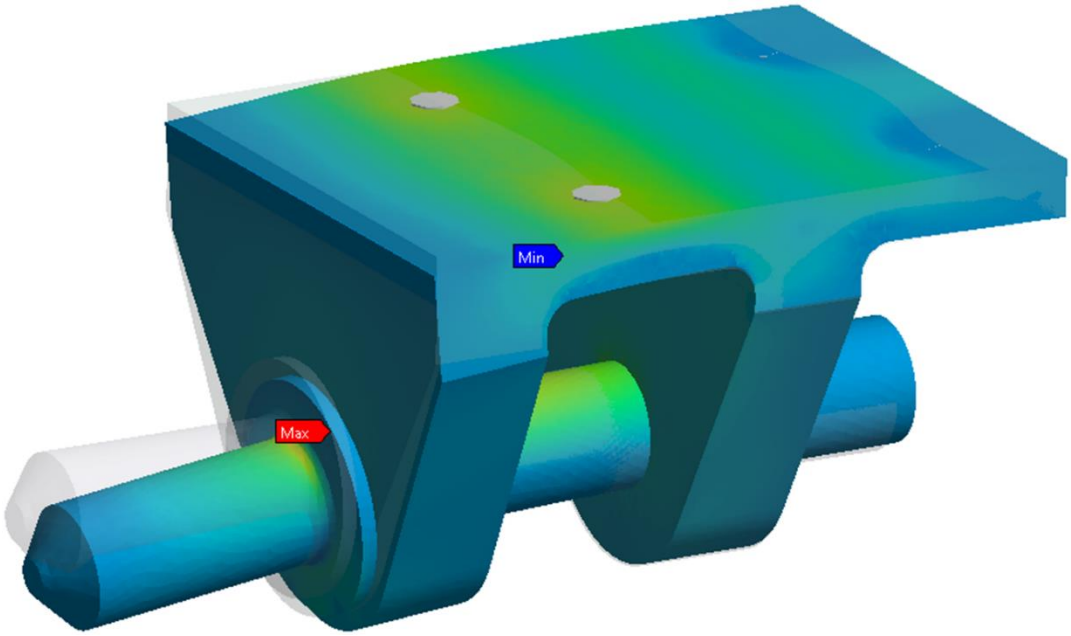

Figure 4.16 Maximum principal stress distribution on extended double wall eccentric pin

As detailed in Figure 4.17, there is quite significant difference between double wall

and double wall extended eccentric pin structures compared to fixed wall eccentric pin solution. The single wall eccentric pin solution has the highest maximum principal stress on front fastener area.

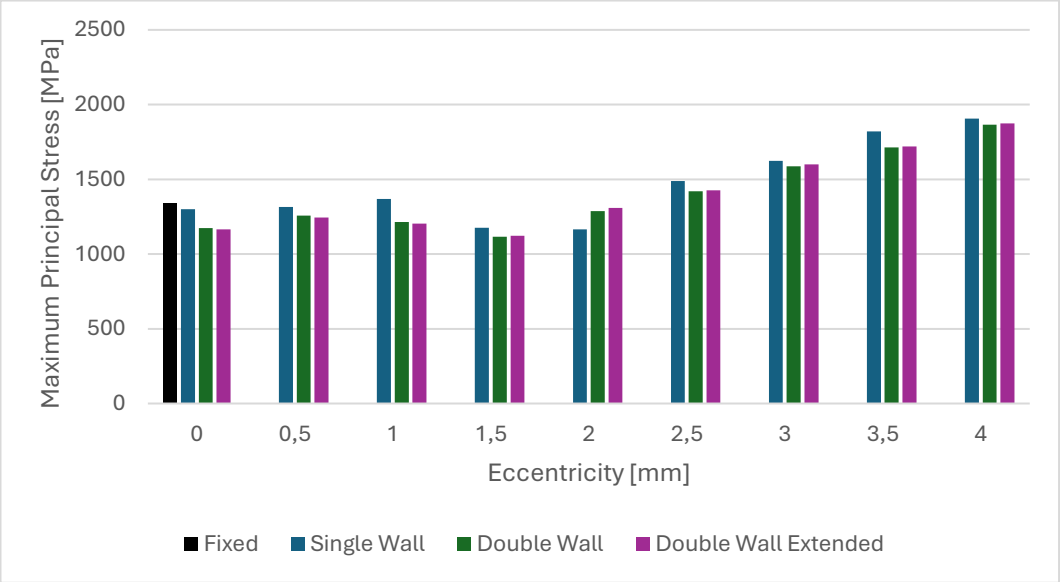

Figure 4.17 Maximum principal stress distribution based on eccentricity levels for pin structure

As illustrated by the Figure 4.18, the maximum principal stress level was significantly lower for the double wall designs compared to the single wall designs. Thanks to the double wall design, which effectively distributes loads and creates a more uniform load path on the housing structure, significantly lower stress levels are achieved. The same reduction in stress is observed with von-Mises stresses for double wall supported housing parts. This demonstrates that the double wall design plays a pivotal role in reducing stress levels in structures.

Similar to von-Mises stresses, different levels of eccentricity can significantly impact the stress distribution in both the pin and the housing surfaces. Changed load distribution due to varying eccentricity levels may affect stress distribution in both the pin and housing structures.

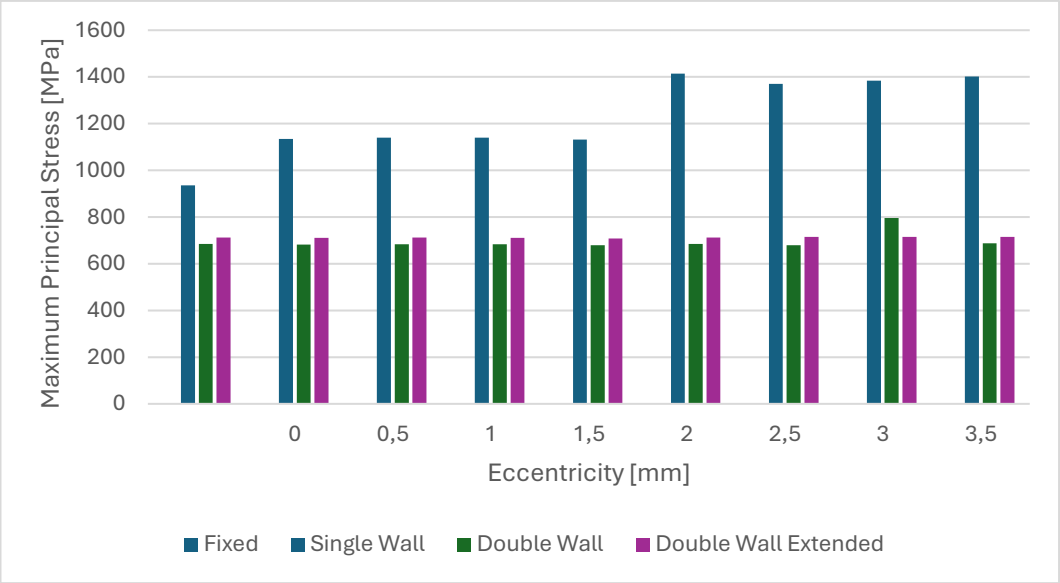

Figure 4.18 Maximum principal stress distribution based on eccentricity levels for housing structure

4.4 Maximum Shear Stresses

The maximum shear stress remained constant under all conditions. No significant stress differences were observed among the design solutions except double wall housing structures.

Table 4.4 Maximum shear stress values based on design

Parameter	Fixed	Single Wall	Double Wall	Extended Double Wall
Maximum Shear Stress Pin [MPa]	649,96	682,76	206,75	208,13
Maximum Shear Stress Housing [MPa]	-	611,71	116,47	77,35

In Figure 4.19 and 4.20, the Maximum Shear Stress is located on the front fasteners of the fixed and single wall solutions, respectively.

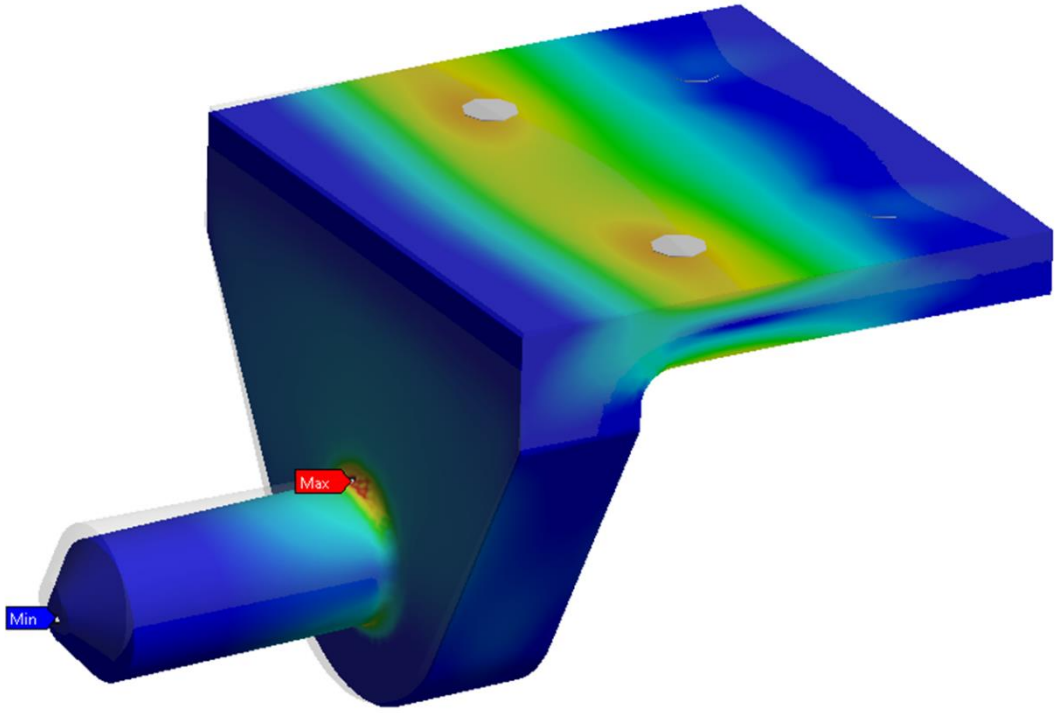

Figure 4.19 Maximum shear stress distribution on fixed pin solution

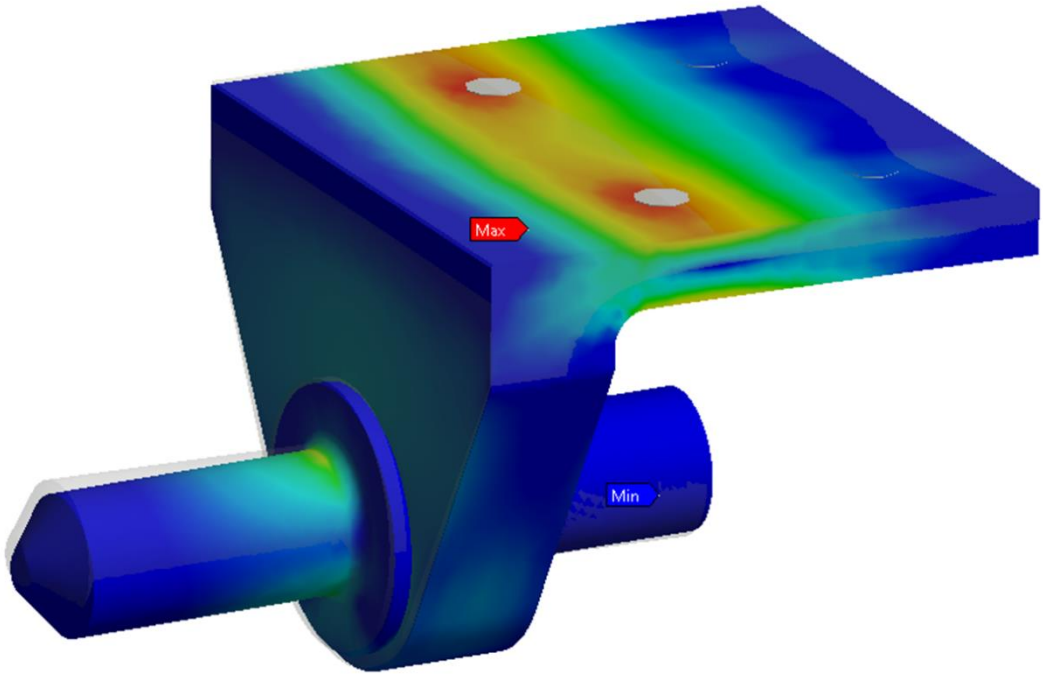

Figure 4.20 Maximum shear stress distribution on single wall eccentric pin

As shown in Figure 4.21 and 4.22, an additional wall and well distributed load, significantly decreased the shear stress on the housing component. Unlike the fixed and single wall design, double wall designs have much lower stress overall of the part.

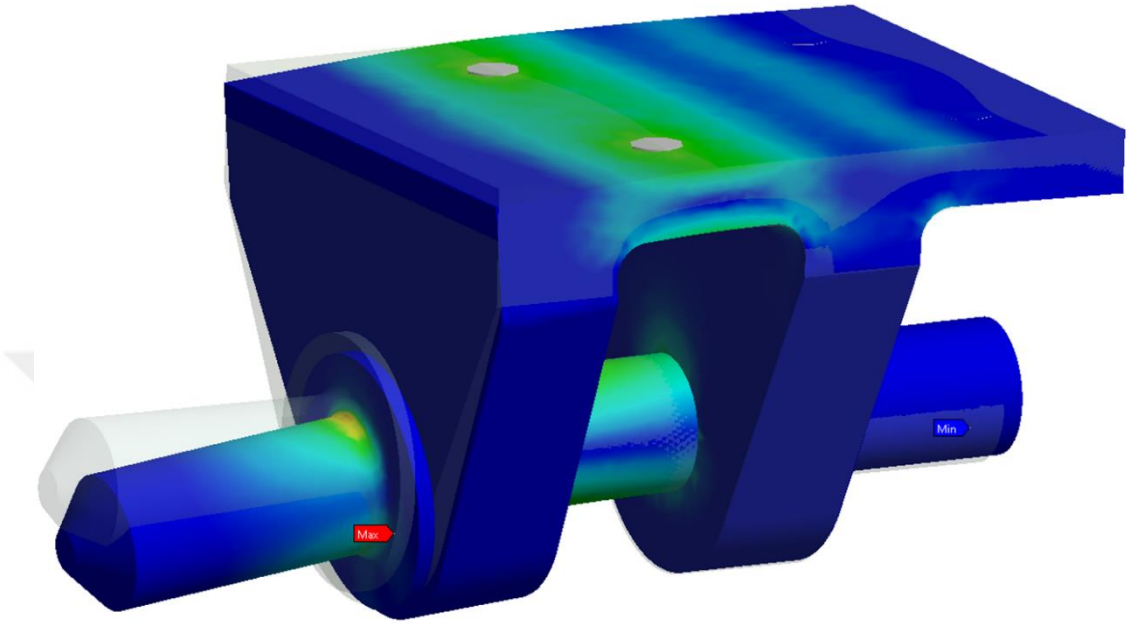

Figure 4.21 Maximum shear stress distribution on double wall eccentric pin

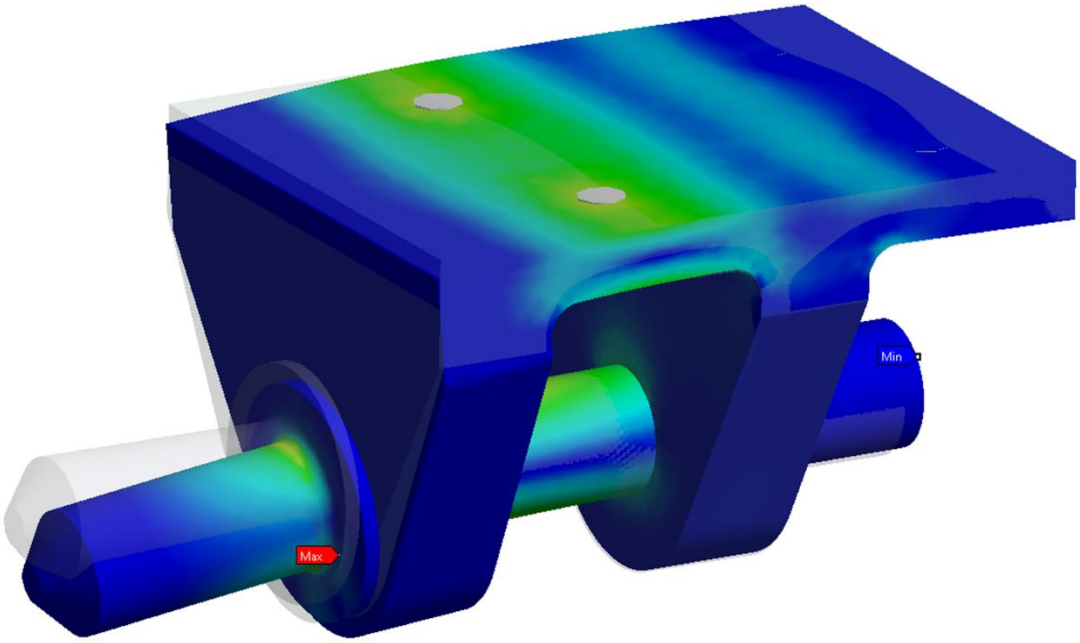

Figure 4.22 Maximum shear stress distribution on extended double wall eccentric pin

Figure 4.23 shows the maximum shear stress distribution and eccentricity effect of the design solutions. As expected, stress values are relatively different for single-wall and double-wall eccentric pin solutions.

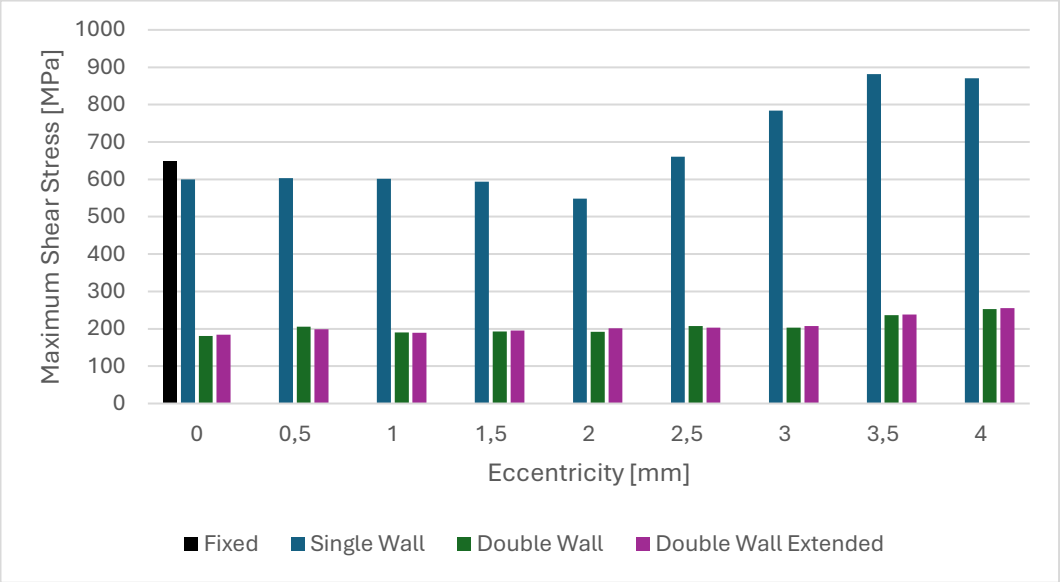

Figure 4.23 Maximum shear stress distribution based on eccentricity levels for pin structure

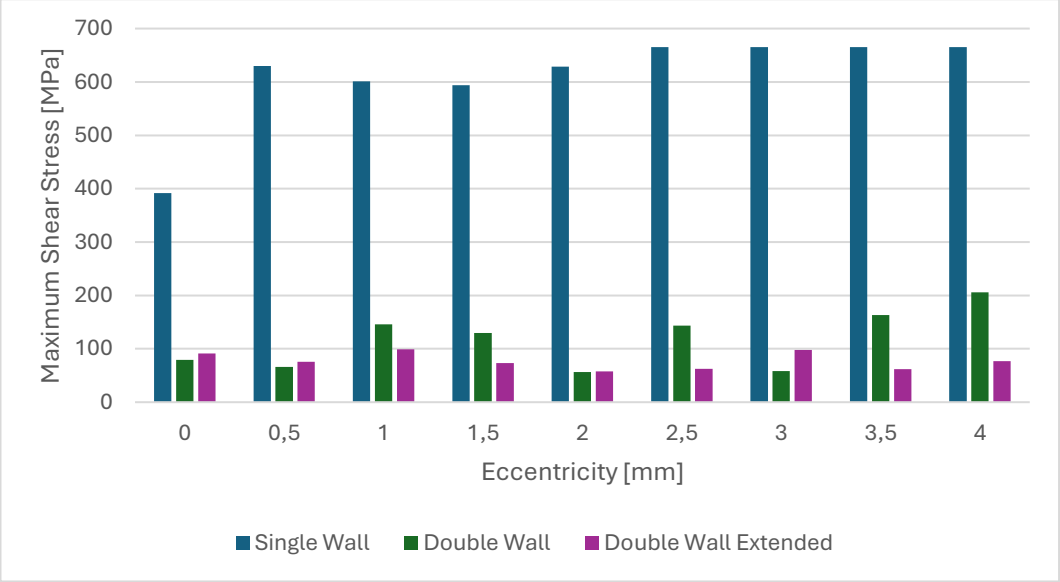

Figure 4.24 Maximum shear stress distribution based on eccentricity levels for housing structure

In contrast, the first-row of fixed and single wall structures presents higher shear stress due to increased stress concentration. As depicted in Figures 4.23 and 4.24, the

additional wall contributes to reduction in shear stress values for both the pin and housing structures, by increasing the surface area. These modifications in stress gradient could have significant implications for the overall structural integrity and longevity of both the pin and housing components.

CHAPTER 5

CONCLUSION

5.1 General Conclusion

The main aim of this study is to present an alternative to canopy locking mechanism. For this purpose, different design solutions designed and carefully analysed. It has been observed that combining additional support into the pin housing structure leads to a substantial reduction in the deflection of the pin structure. This significant decrease in deflection highlights the effectiveness of increasing the support to enhance the structural stability and minimize the displacement under load.

Further analysis revealed that the displacement values in the eccentric pins did not change at the 0-2 mm range of the eccentricity level, however at the 2-4 mm eccentricity stresses increased. The von-Mises and Maximum Shear Stress values were affected by increased eccentricity. This pattern indicates that the relationship between eccentricity levels and the stress experienced by the component does directly correlate with the severity of the loading.

In practical terms, the design of the double wall and extended double wall eccentric pin offers notable advantages. It allows for adjustments in rigid structures, such as canopies, while demonstrating a displacement that is much lower than that of a fixed pin. Such a reduction in displacement is crucial for ensuring flight safety and maintaining cabin pressure reliability. With the displacement remaining below 2 mm, the design contributes to both enhanced safety and effectiveness in maintaining pressure levels within the cabin. On the other hand, decreased peak stress value may lead to total cost of the locking mechanism due to potential changes in the pin housing material. Considerations such as material availability, cost and machinability parameter effects the production cost of the part.

As a result of the study, it was observed that the double wall and extended double wall eccentric pin design proved to be highly advantageous for use in aircraft canopies. The displacement values and loads on the hosing part were significantly reduced in the

double supported designs. Stress levels recorded on the pin were comparable, but all stresses for the eccentric pins were lower than those observed in the fixed pin design. This enables the canopy to operate effectively at higher altitudes, where reduced displacement and minimized pressure loss are critical for optimal performance.

5.2 Recommendations for the Future Work

Fasteners can be modelled with their elastic properties to accurately simulate primary structure connections. While this approach may lead to increase in calculation time, it provides more realistic FEA solutions.

A fatigue study may run to evaluate the replace or maintenance time of the eccentric pin structures. In practical, due to manoeuvre or aerodynamic loads each pin has a different load profile. This load profile may help to calculate failure or maintenance intervals.

Counterpart of the locking mechanism can be modelled for detailed analysis. By considering the contact relationship and mechanism tolerances, a detailed finite element analysis can be performed to understand the impact of the pin's performance.

Coating applications and their friction coefficients for corrosion resistance can be modelled and investigated to understand their effects on displacement and structural forces.

To enhance the efficiency of parametric analysis and streamline data collection, a script code can be developed for the analysis software.

REFERENCES

[1] Petrescu, R. V., Aversa, R., Akash, B., Bucinell, R., Corchado, J., Apicella, A., & Petrescu, F. I., "History of aviation-a short review. Journal of Aircraft and Spacecraft Technology", 1, 30-49, 2017.

[2] Darke D., "The Ottomans: a Cultural Legacy", New York, Thames & Hudson, Inc., 2022.

[3] Sorenson D. S., "An Introduction to the Modern Middle East History, Religion, Political Economy, Politics", Westview Press, 2013.

[4] Wright, O., Kelly, F. C., "How We Invented the Airplane", Philadelphia, McKay, 1953.

[5] Leski, A., Baraniecki, R., & Malachowski, J. (2002). "Numerical Simulation to Study the Influence of the Thickness of Canopy at a Bird Strike", In DS 30: Proceedings of DESIGN, the 7th International Design Conference, 667-672, Dubrovnik, 2022.

[6] Bruyn Neto, M. D., Sales, R. D. C. M., Iha, K., & Rocco, J. A. F. F., "Reinforced Transparencies for Aerospace Application-Case Description", Journal of Aerospace Technology and Management, 8, 49-54, 2016.

[7] Curry M., NASA Dryden T-38A Talon Graphics Collection, Retrieved July 16, 2024, from https://www.dfrc.nasa.gov/Gallery/Graphics/T-38A/index.html, 2006.

[8] Murphy, J. D., & McNiece, M. A., "Military Aircraft, 1919-1945: An Illustrated History of Their Impact", USA: Bloomsbury Publishing USA, 2008.

[9] McCarty R.E., "Finite Element Analysis of a Bird-Resistant Monolithic Stretched Acrylic Canopy Design for the F-16A Aircraft", In Aircraft Systems and Technology Conference, Air Force Wright Aeronautical Labs, Wright- W Patterson AFB, 1981.

[10] Coombs L.F.E., "Control in the Sky: the Evolution and History of The Aircraft Cockpit", United Kingdom: Pen & Sword, 2005.

[11] Lampietro, P. F., "Operational Roles, Aircrew Systems and Human Factors in Future High Performance Aircraft", Aerospace Medical Panel's Specialists' Meeting, Lisbon, Portugal, 22-26 October, 1979.

[12] MIL-STD-850B, Military Standard, "Aircrew Station Vision Requirements for Military Aircraft", November 1970.

[13] Lawrence Jr, J. H., “Guidelines for the Design of Aircraft Windshield/Canopy Systems", In AFWAL-TR-80-3003., Wright Patterson Air Force Base Ohio, 1980.

[14] Dixon R., Moats S., Rhemann J., Patterson J., and others. “Don't Let Your Phantom Blow”, Tac Attack, *Volume 16 Number 5*, 4-6. Retrieved May 14, 2024, https://www.acc.af.mil/Portals/92/Docs/ACC%20SAFETY/COMBAT%20EDGE/TAC76_05.pdf. May 1976.

[15] Langley Air Force Base Briefing: F-22 03-041 Stuck Canopy, https://spaceref.com/status-report/langley-air-force-base-briefing-f-22-03-041-stuck-canopy/, May 18, 2024.

[16] Langley Air Force Base Briefing: F-22 03-041 Stuck Canopy, Retrieved May 22, 2024, from https://spaceref.com/status-report/langley-air-force-base-briefing-f-22-03-041-stuck-canopy, April 24, 2006.

[17] AAIB Report: Extra NG, G-MIIL, Retrieved 24 May 2024, from https://assets.publishing.service.gov.uk/media/65d61630188d77001103883c/Extra-NG_G-MIIL_04-24.pdf, 2022.

[18] Final Report SERIOUS INCIDENT/2022/1097, Retrieved May 24, 2024, https://pkbwl.gov.pl/wp-content/uploads/2023/01/2022_1097_RK_EN.pdf, 18 March 18, 2022.

[19] Bathie, C. W., “Locking and Actuating Mechanisms for Aircraft Canopies”, PATENT, U.S. Patent No. 3,006,583. Washington, DC: U.S. Patent and Trademark Office, 1961.

[20] NICHOLS, G., “Aircraft Canopy Lock”, Patent Number Us-Patent-4, 283, 995; Us-Patent-Appl-Sn-847276; Us-Patent-Class-91-410; Us-Patent-Class-91-325; Us-Patent-Class-91-341, 1981.

[21] Shen, L., Zhang, Y., Song, K., & Song, B., “Failure Analysis of a Lock Mechanism with Multiple Dependent Components Based on Two-Phase Degradation Model”. Engineering Failure Analysis, 104, 1076-1093. 2019.

[22] Jasiński, W., Krysiak, P. & Pichlak, C., “Locking Mechanism of a Slider with Self-Adjusting Backlash: Design and Dynamic Analysis”, Materials Research Proceedings, 24, 2022.

[23] JSSG-2006. “Jointly Apply Specification Guide of U.S. Ministry of National Defense”, 2006.

[24] EASA, C., “Certification Specifications for Large Aeroplanes”, CS 25, 1970, 2007, 2009.

[25] NATO, “Introduction to Flight Test Engineering, Flight Test Techniques Series”, 14, 2005.

[26] NASA Engineering and Safety Center , “F/A-18 and E/A-18 Fleet Physiological Episodes,” Technical Assessment Report, NESC-RP-17-01205, 1, September 14, 2017.

[27] Arunachalam, S., & Varadappan, A. M. S., “Effect of Supply Air Failure on Cabin Pressure Control System of a Fighter Aircraft”, International Journal of Aeronautical and Space Sciences, 24(2), 570-580. 2023.

[28] F/A-18 Hornet (Tactical), Retrieved May 28, 2024, https://www.history.navy.mil/content/history/museums/nnam/explore/collections/aircraft/f/f-a-18-hornet--tactical-.html.

[29] Srinivasan, R. S. A., “Theoretical Framework for Functional Form Tolerances in Design for Manufacturing”, The University of Texas at Austin, 1994.

[30] Inflatable Canopy Seals, Retrieved August 12, 2024, https://kirkhill.com/products/defense/inflatable-canopy-seals.

[31] Inflatable Seals Product Catalogue, Retrieved August 14, 2024, https://www.westernrubbers.com/wp-content/uploads/2023/06/Inflatable-Seals_Digital_2023.pdf.

[32] Trelleborg Sealing Solutions Airseal, Retrieved August 14, 2024, https://www.trelleborg.com/-/media/tss-media-repository/tss_website/pdf-and-other-literature/catalogs/airseal_gb_en.pdf.

[33] First U.S. Marine Pilots Lockheed Martin F-35, Retrieved August 14, 2024, https://www.thenorthspin.com/news09/031909lockheed.html, 2009.

[34] https://media.defense.gov/2010/Aug/09/2000336086/-1/-1/0/100715-F-6175D-319.JPG, Retrieved February 8, 2024.

[35] Jiang, D., Chen, T., Xie, J., Cui, W., & Song, B., “A Mechanical System Reliability Degradation Analysis and Remaining Life Estimation Method - With the Example of an Aircraft Hatch Lock Mechanism”. Reliability Engineering & System Safety, 230, 108922, 2023.

[36] American Fighter - 22A Raptor, Американский истребитель, https://nevsepic.com.ua/aviaciya/13403-amerikanskiy-istrebitel-22a-raptor-82-foto.html, August 16, 2024.

[37] A 360-Degree Look at the Interior of the J-20 Cockpit Shows That the Details are Still Insufficient, Retrieved from http://k.sina.cn/article_1407590812_53e6219c00100qknx.html, August 10, 2024.

[38] Moniruzzaman, F. M., Nasiri, A., & Hadadzadeh, A., “Evading Strength-Ductility Trade-Off in Directed Energy Deposited Precipitation Hardenable Stainless Steels: A Pathway Through Precipitation Kinetics Modeling, Design of Heat Treatment, and Evolution of Clusters”, Materials Today Communications, 35, 2023.

[39] United States. Dept. of Defense., “Military Handbook: Metallic Materials and Elements for Aerospace Vehicle Structures”, 1, US Department of Defense, 1990.

[40] Hochanadel, P. W., Edwards, G. R., Robino, C. V., & Cieslak, M. J., “Heat treatment of Investment Cast PH 13-8 Mo Stainless Steel: Part I. Mechanical properties and Microstructure.” Metallurgical and Materials Transactions A, 789-798, 1994.